ChemPubSoc Europe

DOI: 10.1002/cctc.201500197

CHEMCATCHEM Full Papers

Insights into the Oxidation State and Location of Rhenium in Re-Pd/TiO_2 Catalysts for Aqueous-Phase Selective Hydrogenation of Succinic Acid to 1,4-Butanediol as a Function of Palladium and Rhenium Deposition Methods

Bao Khanh Ly,[a] Benoît Tapin,[b] Mimoun Aouine,[a] Pierre Delichere,[a] Florence Epron,[b] Catherine Pinel,[a] Catherine Especel,*[b] and Michèle Besson*[a]

This paper is dedicated to Dr. Daniel Duprez and Dr. Pierre Gallezot with whom we have shared many discussions about supported (bi)metallic catalysts.

ReO_x-Pd/TiO_2 catalysts prepared from different 2 wt%Pd/TiO_2 catalysts using two protocols for the deposition of the Re promoter (successive impregnation and catalytic reduction) were characterized by different techniques to better understand the nature of the active and selective sites implied in the aqueous-phase hydrogenation of succinic acid to 1,4-butanediol. Regardless of the support and Re introduction method, it was established that varying amounts of Pd and Re were in very close proximity without electronic interaction in the reduced catalysts. A high fraction of Re always remained partially oxidized to generate a bimetallic catalyst that can provide the necessary bifunctional sites to enable the selective hydrogenolysis of the intermediate γ-butyrolactone to 1,4-butanediol. Depending on the method of promotion, the ReO_x species that interact with Pd were deposited as clusters with different spatial Re–Re interactions.

Introduction

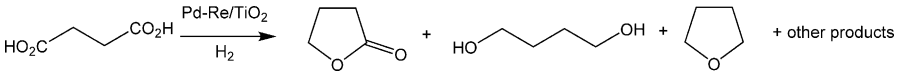

Scheme 1. Catalytic hydrogenation of SUC to BDO.

Succinic acid (SUC; IUPAC name: butanedioic acid) is a petrochemical intermediate that is currently produced by the catalytic hydrogenation of maleic anhydride to succinic anhydride and subsequent hydration or by the catalytic hydrogenation of maleic acid. After it was the focus of many research biotechnological projects in the last decade, bio-based SUC is now produced by fermentation in a sustainable and highly efficient manufacturing process using renewable biomass as the feedstock and metabolically engineered micro-organisms.[1,2] SUC has been identified as one of the most important platform chemicals in biorefinery, which will one day replace petroleum refinery.[3,4] SUC has a wide range of industrial applications.[5] It can be converted readily by catalytic hydrogenation to other important bulk chemicals, such as 1,4-butanediol (BDO), THF, and γ-butyrolactone (GBL; Scheme 1). In particular, BDO, which was until recently manufactured entirely from petroleum-based feedstocks, is an important commodity chemical that is used to manufacture large amounts of plastics and important polymers such as polyesters, polyurethanes, and spandex elastic fibers. A variety of catalysts have been described extensively in patents for the catalytic hydrogenation reaction of maleic acid, maleic anhydride, and SUC to BDO. The most frequently used active and selective catalysts for this reaction comprise a noble metal in combination with another metal such as Re or Sn. These reactions are conducted predominantly in the gas phase or in organic solvent.[6,7] The use of a series of monometallic Pd, Ru, and Re catalysts supported on different carbon materials has been reported for the liquid-phase hydrogenation of SUC to THF in dioxane at 240 °C under 60 bar.[8–13] Bimetallic Re–Ru catalysts showed selectivity to BDO at 200 °C under 80 bar in dioxane.[14]

However, there are few examples of the hydrogenation of SUC in an aqueous solution,[15–21] an important medium in the conversion of compounds obtained from renewable resources

[a] Dr. B. K. Ly, Dr. M. Aouine, Dr. P. Delichere, Dr. C. Pinel, Dr. M. Besson
Institut de recherches sur la catalyse et l'environnement de Lyon (IRCELYON)
UMR CNRS-Université Lyon1
2 Avenue Albert Einstein, 69626 Villeurbanne Cedex (France)
Fax: (+33) 04-72-44-53-99
E-mail: michele.besson@ircelyon.univ-lyon1.fr

[b] Dr. B. Tapin, Dr. F. Epron, Dr. C. Especel
Institut de Chimie des Milieux et des Matériaux de Poitiers (IC2MP)
UMR CNRS-Université Poitiers
4 rue Michel Brunet, TSA 51106, 86073 Poitiers Cedex 9 (France)
Fax: (+33) 05-49-45-37-41
E-mail: catherine.especel@univ-poitiers.fr

Supporting information for this article is available on the WWW under http://dx.doi.org/10.1002/cctc.201500197.

This publication is part of a Special Issue on Palladium Catalysis. To view the complete issue, visit: http://onlinelibrary.wiley.com/doi/10.1002/cctc.v7.14/issuetoc

processing.[4] The harsh operating temperatures usually used (up to 240 °C) favored the formation of THF and selectivity to BDO was limited.[15–17] However, we have reported the aqueous-phase hydrogenation of SUC to BDO at 160 °C under 150 bar using Re-Pd catalysts supported on carbon or TiO_2.[18–20] Monometallic Pd catalysts were totally unselective to BDO and produced mostly GBL.[21] If only Re was present, no reaction was observed in water. In turn, bimetallic catalysts that combine both metals, namely, Re deposited on Pd catalysts, have demonstrated the possibility to tune the reaction selectivity towards BDO. We have also observed the effects of the method of preparation of the Pd catalyst, by the method of introduction of the Re precursor over the monometallic Pd catalyst, and by the Re loading. The results indicated that the catalysts prepared by a simple successive impregnation method (SI) required a significantly higher amount of Re compared with the catalysts prepared by catalytic reduction deposition (CR) to obtain a high yield of BDO. However, the SI-prepared Pd-Re catalysts exhibited a higher selectivity to BDO.

Such a marked effect on catalyst selectivity might be because of the different locations of the Re additive or the degree of contact between the promoter and Pd. Systematic studies on the characterization of the two-component catalysts and the interpretation of the action of the Re promoter associated with the noble metal on the activity and selectivity of this reaction are rather scarce.[14,20] As an example, characterizations of a series of Re-Ru catalysts supported on mesoporous carbon (MC) after incipient wetness coimpregnation of metal precursors in acetone showed the formation of a Re-Ru miscible phase during the reduction process at 500 °C.[14] The reducibility, metal dispersion, and oxidation state were influenced strongly by the Re/Ru molar ratio. The 0.3Re-0.2Ru/MC catalyst showed the highest turnover frequency (TOF) for the formation of BDO in dioxane, which was correlated to the largest amount of weak hydrogen binding sites determined by H_2 temperature-programmed desorption (TPD).

In a recent paper,[20] we compared the physical and chemical properties of two Re-Pd bimetallic catalysts synthesized from a given 2 wt%Pd/TiO_2 monometallic catalyst (which was prepared by an impregnation method in an acidic aqueous medium using $PdCl_2$ as the precursor salt) either by CR or by SI. This study gave us some partial information on the Re promoter and suggests a different localization of the Re deposit and a different oxidation degree of the Re species depending on the introduction mode. However, the mechanism that underlies the effect of Re on the tuning of the catalyst selectivity to the desired pathway was not resolved. As different interactions between the Pd precious metal and the Re promoter may be expected that depend on the deposition method, we thought it was necessary to characterize a larger set of catalysts. For that purpose, Re was introduced on three different monometallic catalysts and the resulting bimetallic solids were characterized thoroughly to provide further insights into the Re species present, their different oxidation states, their location relative to the Pd particles, and the interactions between both metals and with the support to try to explain the differences in the catalytic performances observed. In this study, the catalysts were characterized extensively using various techniques such as XRD, TEM, X-ray photoelectron spectroscopy (XPS), temperature-programmed reduction (TPR), H_2 chemisorption, and the gas-phase model reaction of cyclohexane dehydrogenation, a structure-insensitive reaction catalyzed by Pd active sites. The characterizations were correlated tentatively to the catalytic results observed.

Results

XRD and TEM characterizations

Pd and Re monometallic catalysts

The three monometallic Pd parent catalysts used in this study (2 wt%Pd_{Cl}/P25, 2 wt%Pd_{KCl}/P25, and 2 wt%Pd_{KCl}/DT51) have been described previously for the selective hydrogenation of SUC to GBL and some of their characteristics have been shown.[21]

The Pd catalysts showed no XRD peaks other than those of rutile or/and anatase, which indicated a high dispersion of Pd in all prepared samples. The highest dispersion measured from H_2 chemisorption (33%) was obtained for the catalyst prepared by the impregnation of the $PdCl_2$ salt (2 wt%Pd_{Cl}/P25), whereas the deposition–precipitation method that involves K_2PdCl_4 afforded dispersions of 15 and 27% for 2 wt%Pd_{KCl}/P25 and 2 wt%Pd_{KCl}/DT51, respectively. By TEM, the 2 wt%Pd_{Cl}/P25 catalyst showed a homogeneous Pd distribution with particles that were mainly between 1 and 2 nm in diameter (average particle size 1.8 nm).[21] The Pd particles in 2 wt%Pd_{KCl}/DT51 were also dispersed homogeneously on the solid with diameters between 1.5 and 3 nm (average particle size 2.4 nm; Figure S1). The average metal particle sizes determined by TEM for 2 wt%Pd_{Cl}/P25 and 2 wt%Pd_{KCl}/DT51 (1.8 and 2.4 nm, respectively) were slightly smaller than those deduced from H_2 chemisorption (2.8 and 3.5 nm, respectively).[21]

In the XRD pattern of 1.9 wt%Re_{pH1}/P25 and 3.1 wt%Re_{pHn}/DT51 monometallic Re catalysts, the peaks that correspond to metallic Re or ReO_x species were not detected at all, which indicates the high dispersion of the Re species. It was difficult to detect Re particles in the TEM images of 1.9 wt%Re_{pH1}/P25 (Figure S2). Only very scarce support particles showed the presence of highly dispersed nanoparticles (< 0.7 nm). However, the environmental transmission electron microscopy (ETEM) pictures in the scanning transmission electron microscopy (STEM) mode of 3.1 wt%Re_{pHn}/DT51 were able to show very small and uniform Re nanoclusters (< 0.7 nm) on the support (Figure 1). These observations are consistent with the literature. Re in 1.05 wt%Re/Al_2O_3 reduced at 550 °C existed as very small clusters (< 1 nm) that were undetectable by TEM.[22] Very few nanoparticles with a size of 1 nm or less could be observed in Re/TiO_2.[23]

Re-Pd bimetallic catalysts

No discrete Pd- or Re-containing phase was evidenced in the XRD patterns of any of the Re-Pd bimetallic catalysts, which is

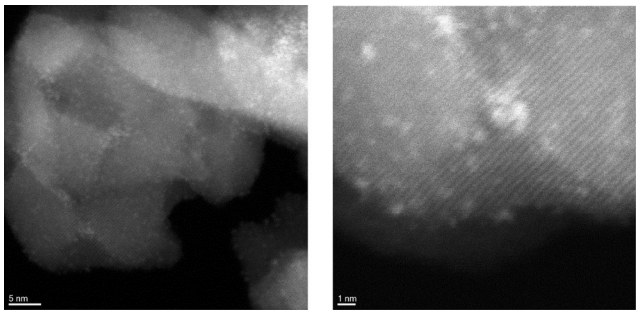

Figure 1. Representative ETEM pictures of 3.1 wt%Re_{pHn}/DT51 in HAADF-STEM mode. Left: scale bar = 5 nm; right: scale bar = 1 nm.

likely because the crystallites are too small to exhibit diffraction patterns (Figure S3).

TEM and STEM images were obtained for some "as-prepared" Re-Pd samples (after reduction and passivation) and energy-dispersive X-ray (EDX) analysis was used to investigate the compositions on small- and large-area scans. The observation was difficult and gave only semiquantitative results as exposure to the stationary electron beam during EDX resulted in the severe degradation of the exposed area. Images and scan areas of two bimetallic catalysts prepared from 2 wt%Pd_{KCl}/DT51 using the CR and SI protocols, 0.8 wt%Re-Pd_{KCl}/DT51-CR and 3.4 wt%Re-Pd_{KCl}/DT51-SI, respectively, are shown in Figures S4 and S5.

In 0.8 wt%Re-Pd_{KCl}/DT51-CR, most of the particles were highly dispersed with a diameter in the range 1–3 nm, which is not significantly different from that in the monometallic parent (Figure S4). The particles analyzed contained only Pd, and no detectable Re content was evidenced by EDX analysis (Figure S4a). An area was found to contain a very large agglomerate of Re with a diameter of around 1 μm (Figure S4b). However, this large particle was isolated, and it does not exclude the possibility that the majority of Re was still well dispersed in the solid. This was rather surprising if we consider that the CR method should deposit Re selectively on Pd. An explanation for this unexpected distribution could find its origin in experimental problems encountered during the preparation of this solid from Pd_{KCl}/DT51 by CR. Indeed, the very fine granulation of this support caused plugging of the frit and an inhomogeneous hydrogen flow, which could have disturbed the deposition of the promoter during preparation.

In 3.4 wt%Re-Pd_{KCl}/DT51-SI, which has a high Re content, small particles in the range 1–2 nm were also detected (Figure S5). EDX analysis on large zones (50 nm) detected both Pd and Re with a mass ratio of Re/Pd = 2.03 close to the ratio of 1.75 determined by inductively coupled plasma optical emission spectroscopy (ICP-OES; Figure S5). Several spot elemental analyses with the beam concentrated on isolated particles showed that they contained either Pd or both Pd and Re, with Re/Pd mass ratios that varied considerably among the particles analyzed and that were lower than the global mass ratio. This 3.4 wt%Re-Pd_{KCl}/DT51-SI catalyst and the corresponding parent catalyst were analyzed in the STEM mode with the annular dark-field detector (ADF-STEM). The images displayed in Figure 2 show evidence of well-dispersed particles in both solids. However, as the contrast and the particle sizes were very similar, it was not possible to draw conclusions on the respective localization of Re or Pd. Some TEM pictures of the catalysts prepared from 2 wt%Pd_{KCl}/P25 loaded with 0.6 or 2.9 wt% Re by CR show well-dispersed metallic particles (Figure S6).

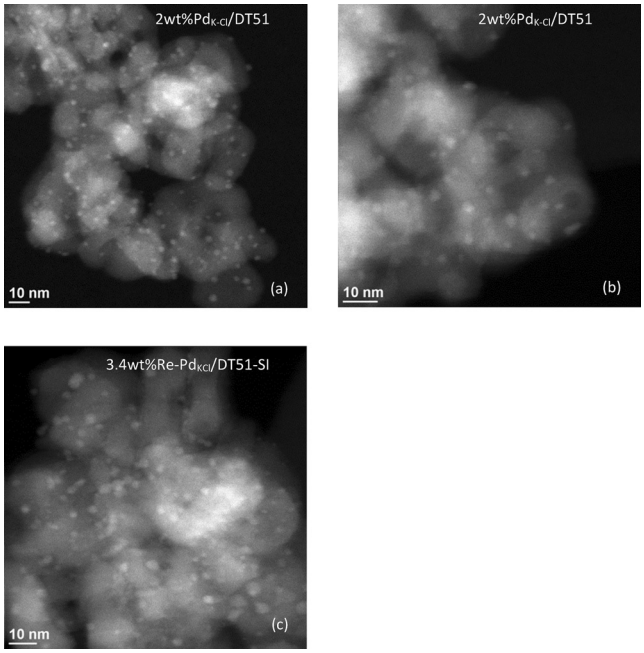

Figure 2. Representative HAADF-STEM images of a, b) 2 wt%Pd_{KCl}/DT51 and c) 3.4 wt%Re-Pd_{KCl}/DT51-SI.

Analysis of 1.5 wt%Re-Pd_{KCl}/P25-CR performed using the ETEM instrument in TEM and high-angle annular dark-field scanning transmission electron microscopy (HAADF-STEM) mode is shown in Figure 3. The TEM images showed the presence of Pd particles (Figure 3a). However, the Re clusters were so small that they were not observable. EDX analysis detected mainly Pd associated with some Re (Figure S7, TEM EDX 1–3) and some zones that contained only Re (Figure S7, TEM EDX 4). In HAADF-STEM mode, the images confirmed that Re was dispersed atomically all over the catalyst surface (Figure 3b and c).

Finally, TEM characterization of the bimetallic catalysts prepared from 2 wt%Pd_{Cl}/P25 has been described previously for solids that contain 0.9 and 3.5 wt% Re deposited by CR and SI, respectively.[20] The bimetallic catalyst loaded by CR with 0.9 wt% Re showed metallic particles that were evidently larger than that on the bimetallic catalyst prepared by SI that contained 3.5 wt% Re. The average particle size of these solids was determined to be 5.3 and 2.5 nm, respectively, which can be compared with the parent Pd catalyst average particle size of 1.8 nm. Re was detected on the Pd particles (Figure S7, STEM EDX).

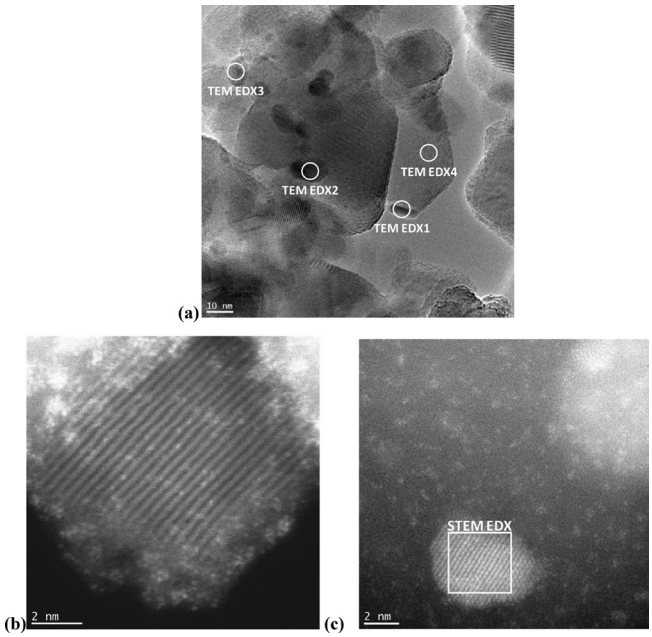

Figure 3. ETEM pictures of 1.5 wt%Re-Pd_{KCl}/DT51in a) TEM (scale bar = 10 nm) and b, c) HAADF-STEM mode (scale bars = 2 nm). The EDX analysis is shown in Figure S7.

XPS

XPS could provide valuable information about the oxidation states of the various species present in the monometallic Re and Pd and bimetallic Pd-Re catalytic systems. The measurements were performed (i) for the monometallic Re catalyst, either after in situ activation with H_2 at 450 °C of the precursor or "as-prepared", that is, reduced at 450 °C and then handled under ambient conditions, (ii) for the parent monometallic Pd catalysts, either "as-prepared", or following in situ reactivation with H_2 at 300 °C, or (iii) for the two-component solids, either after in situ reduction of the precursor at 450 °C for 3 h, "as-prepared", or after in situ rereduction. Some curve-fitting results (binding energy of Pd $3d_{5/2}$ and Re $4f_{7/2}$, distribution of the oxidation states) are summarized in Table 1. The Re/Pd, Pd/Ti, and Re/Ti ratios could be calculated from the surface atomic compositions by taking into consideration the sensitivity factors of the elements. The explored depth by XPS is approximately 3–5 nm. Thus, this analysis may be considered as quite representative of the bulk composition because of the small particle size of the metallic particles in all of the catalysts studied. Globally, after reduction Pd was present in the metallic state and also as Pd^{2+} and Pd^{4+}; several oxidation states were observed for Re, and the situation was more complex.

Re monometallic catalyst

The Re $4f_{7/2}$ spectra of solid 1.9%$[NH_4ReO_4]_{pH1}$/P25 after impregnation with ammonium perrhenate, drying, and in situ reduction at 450 °C, the "as-prepared" catalyst, that is, handled under ambient conditions after synthesis, and then after reactivation at 450 °C under H_2 are illustrated in Figure 4.

Following the reduction of the precursor at 450 °C (Figure 4a), fitting of the Re $4f_{7/2}$ envelope resulted in the identification of two Re components: one with a binding energy (BE) of 40.7 eV, which matches closest with Re^0 with an atomic concentration of 89%, and a second one at BE = 41.5 eV, which was attributed to Re^{3+} (atomic concentration 11%; Table 1, entry 1).[24] As a result of the high oxygen affinity of Re, it was expected that handling in ambient air would cause the oxidation of surface Re. Indeed, after subsequent air exposure of the reduced solid (Figure 4b), Re was reoxidized and the "as-prepared" catalyst then contained a mixture of oxidized Re species with 17% Re^{4+} (BE = 43.1 eV), 44% Re^{6+} (BE = 44.2 eV), and 39% Re^{7+} (BE = 46.2 eV; Table 1, entry 2). However, after a new in situ hydrogen treatment (Figure 4c), only 15% Re was in the zero-valent state, and the remainder was Re^{3+} (Table 1, entry 3). This indicates that different Re species that can be oxidized to various degrees are present and coexist on the support surface.

Furthermore, the Re/Ti atomic ratio initially determined at 0.196 in the solid reduced at 450 °C (Figure 4a) decreased substantially to 0.054 and 0.049 (Table 1, entries 1–3), respectively, after air exposure (Figure 4b) and subsequent rereduction (Figure 4c). In addition, in measurements of the reactivated solid, the BEs of Re^0 and Re^{3+} were 0.2 eV lower than that in the freshly reduced sample. Both observations indicate some agglomeration of Re particles on the surface, which could be attributed to the presence of moisture during the reduction step.[25] It is highly probable that nanoclusters or monoatomic Re species exist in the initially reduced catalysts as proposed and evidenced on alumina and TiO_2.[25–28] After exposure to air, Re was detected by TEM as very small particles with a size < 0.7 nm in the "as-prepared" sample (Figure S2 and Figure 1).

Pd monometallic catalysts

After synthesis and storage in air, the fitting of the Pd envelope for the 2 wt%Pd_{KCl}/DT51 "as-prepared" monometallic catalyst resulted in the identification of Pd^0 (82%, Pd $3d_{5/2}$ BE = 335.2 eV) and a minor amount of oxidized Pd^{2+} species (15%, BE = 336.9 eV) and Pd^{4+} (3%, BE = 338.0 eV; Table 1, entry 4). After the solid was reactivated in H_2 at 300 °C, Pd was nearly completely reduced to the zero-valent state (95% Pd^0 and 5% Pd^{2+}; Table 1, entry 5). The "as-prepared" Pd_{Cl}/P25 contained Pd^0 (34%, BE = 335.3 eV) and Pd^{2+} (66%, BE = 337.0 eV; Table 1, entry 16). In the same way, reactivation at 450 °C reduced Pd totally to the zero-valent state (100% Pd^0, BE = 335.0 eV; Table 1, entry 17). Pd_{KCl}/P25 was not analyzed but similar results may be expected, that is, reduction to mainly Pd^0.

Re-Pd bimetallic catalysts prepared by SI from Pd_{KCl}/DT51 and Pd_{KCl}/P25

The Pd and Re spectra of the bimetallic 2.6wt%Re-Pd_{KCl}/DT51-SI and 2.7 wt%Re-Pd_{KCl}/P25-SI catalysts, which were prepared by SI of the Pd_{KCl}/DT51 and Pd_{KCl}/P25 parent catalysts, were analyzed after their synthesis and then "as-prepared", that is, following exposure to air. As an illustration, the spectra of Pd

Table 1. XPS data (BEs of the Re $4f_{7/2}$ and Pd $3d_{5/2}$ components, distribution of Pd and Re oxidation states, surface atomic ratios).

Entry	Catalyst	Treatment	XPS data Pd $3d_{5/2}$ BE[a] [eV] ([%] Pd^{n+})	XPS data Re $4f_{7/2}$ BE[a] [eV] ([%] Re^{n+})	Pd/Ti-Re/Ti-Re/Pd (atomic ratio)	$(Re/Pd)_{bulk}$[d] (atomic ratio)
1	1.9%$[NH_4ReO_4]_{pH1}$/P25	reduction[b]		40.7 (89 Re^0) 41.5 (11 Re^{3+})	0.196	
2	1.9%Re_{pH1}/P25	"as-prepared"		43.1 (17 Re^{4+}) 44.2 (44 Re^{6+}) 46.2 (39 Re^{7+})	0.054	
3		reduction[b]		40.5 (15 Re^0) 41.3 (85 Re^{3+})	0.049	
4	2%Pd_{KCl}/DT51	"as-prepared"	335.2 (82 Pd^0) 336.9 (15 Pd^{2+}) 338.0 (3 Pd^{4+})		0.042	
5		reduction[b]	335.2 (95 Pd^0) 336.9 (5 Pd^{2+})		0.038	
6	2.6%$[NH_4ReO_4]$-Pd_{KCl}/DT51-SI	reduction[b]	335.2 (100 Pd^0)	40.1 (30 Re^0) 41.2 (70 Re^{3+})	0.032/0.029/0.90	0.77
7	2.6%Re-Pd_{KCl}/DT51-SI	"as-prepared"	335.2 (57 Pd^0) 336.9 (43 Pd^{2+})	43.3 (16 Re^{4+}) 44.2 (41 Re^{6+}) 46.1 (43 Re^{7+})	0.025/0.033/1.32	0.77
8		reduction[b]	335.1 (100 Pd^0)	40.4 (27 Re^0) 41.2 (73 Re^{3+})	0.026/0.036/1.38	
9	1.9%Re-Pd_{KCl}/DT51-CR	reduction[b]	335.1 (95 Pd^0) 336.5 (5 Pd^{2+})	40.0 (30 Re^0) 41.2 (70 Re^{3+})	0.027/0.028/1.04	0.62
10	2%Pd_{KCl}/P25					
11	2.6%$[NH_4ReO_4]$-Pd_{KCl}/P25-SI	reduction[b]	335.0 (100 Pd^0)	40.1 (37 Re^0) 41.3 (63 Re^{3+})	0.028/0.03/1.07	0.74
12	2.7%Re-Pd_{KCl}/P25-SI	"as-prepared"	335.0 (61 Pd^0) 337.0 (39 Pd^{2+})	43.7 (29 Re^{4+}) 44.4 (24 Re^{6+}) 46.2 (47 Re^{7+})	0.038/0.052/1.37	0.77
13		reduction[b]	335.0 (100 Pd^0)	40.1 (34 Re^0) 41.2 (66 Re^{3+})	0.027/0.059/2.18	
14		O_2+reduction[c]	335.1 (100 Pd^0)	40.5 (36 Re^0) 41.5 (64 Re^{3+})	0.027/0.051/1.90	
15	1.5%Re-Pd_{KCl}/P25-CR	reduction[b]	335.4 (92 Pd^0) 336.7 (8 Pd^{2+})	40.2 (74 Re^0) 41.3 (26 Re^{3+})	0.030/0.050/1.69	
16	2%Pd_{Cl}/P25	"as-prepared"	335.3 (34 Pd^0) 337.0 (66 Pd^{2+})		0.065	
17		reduction[b]	335.0 (100 Pd^0)		0.037	
18	0.9%Re-Pd_{Cl}/P25-CR	reduction[b]	335.2 (100 Pd^0)	40.3 (14 Re^0) 41.3 (86 Re^{3+})	0.037/0.028/0.78	0.25
19	1.7%Re-Pd_{Cl}/P25-CR	"as-prepared"	335.1 (66 Pd^0) 336.8 (18 Pd^{2+}) 337.7 (16 Pd^{4+})	43.4 (8 Re^{4+}) 44.3 (29 Re^{6+}) 46.1 (63 Re^{7+})	0.036/0.058/1.61	0.46
20		reduction[b]	335.1 (95 Pd^0) 336.5 (5 Pd^{2+})	41.1 (100 Re^{3+})	0.036/0.066/1.83	

[a] BE: binding energy. [b] In situ reduction at 450 °C. [c] In situ oxidation at 300 °C then reduction at 450 °C. [d] ICP-OES data.

and/or Re of 2.6wt%Re-Pd_{KCl}/DT51-SI are shown in Figure 5: "as-prepared", (Table 1, entry 7), and after reactivation under H_2 at 450 °C (Table 1, entry 8). The catalysts prepared by the same SI method on P25 showed similar profiles (data not shown, quantitative results are given in Table 1, entries 12 and 13).

First, after the introduction of Re by SI impregnation and drying, the solid precursors 2.6 wt%$[NH_4ReO_4]$-Pd_{KCl}/DT51-SI and 2.6 wt%$[NH_4ReO_4]$-Pd_{KCl}/P25-SI were reduced in the XPS treatment cell at 450 °C (Table 1, entries 6 and 11). Only metallic Pd was detected ($3d_{5/2}$ BE = 335.2 and 335.0 eV, respectively). Moreover, the peaks for Pd^0 in the bimetallic solids were observed at the same BEs as those in the monometallic Pd material, which suggests that there is no electronic modification of the surface Pd atoms and that the electronic interaction between Re and Pd on the TiO_2 supports is not very strong. In addition, in both catalysts, the Re spectral fits (not shown) indicated a mixture of Re species with characteristic Re $4f_{7/2}$ BEs of 40.1 and ≈41.2–41.3 eV, which match Re^0 and Re^{3+}, respectively. The proportions were 30% Re^0 and 70% Re^{3+}, and 37% Re^0 and 63% Re^{3+} in the DT51- and P25-supported catalysts, respectively, which demonstrates that Re species under the conditions employed could not be reduced completely to metallic Re.

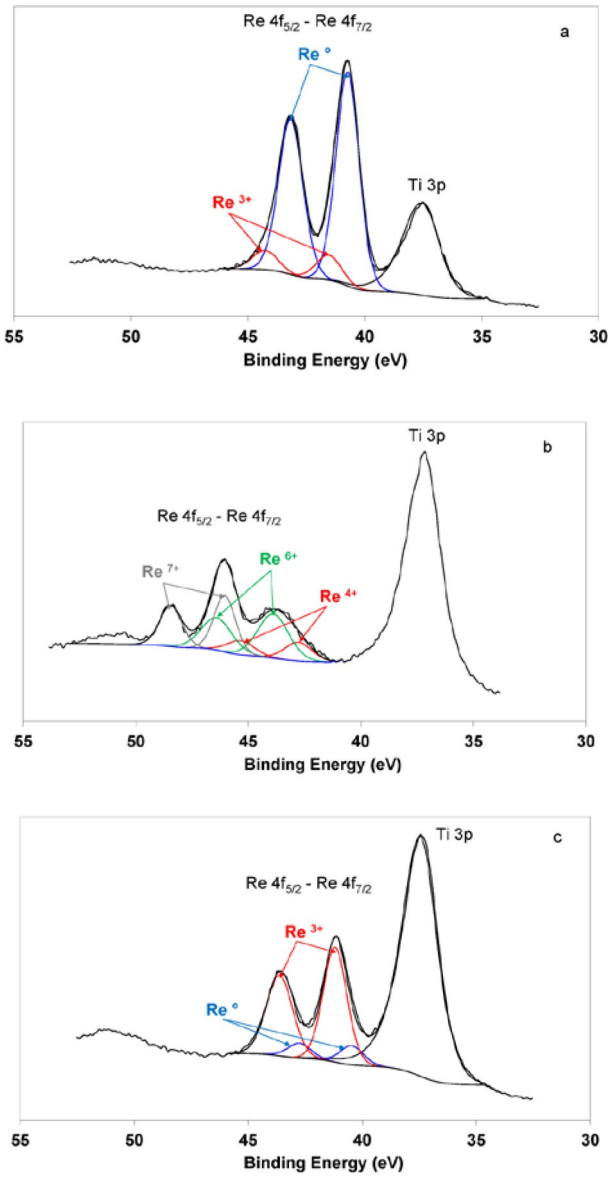

Figure 4. Curve fit to XPS data: Re 4f region of a) 1.9 wt%$[NH_4ReO_4]_{pH1}$/P25 after in situ reduction, b) 1.9 wt%Re_{pH1}/P25 "as-prepared", and c) 1.9 wt%Re_{pH1}/P25 "as-prepared" after in situ reactivation.

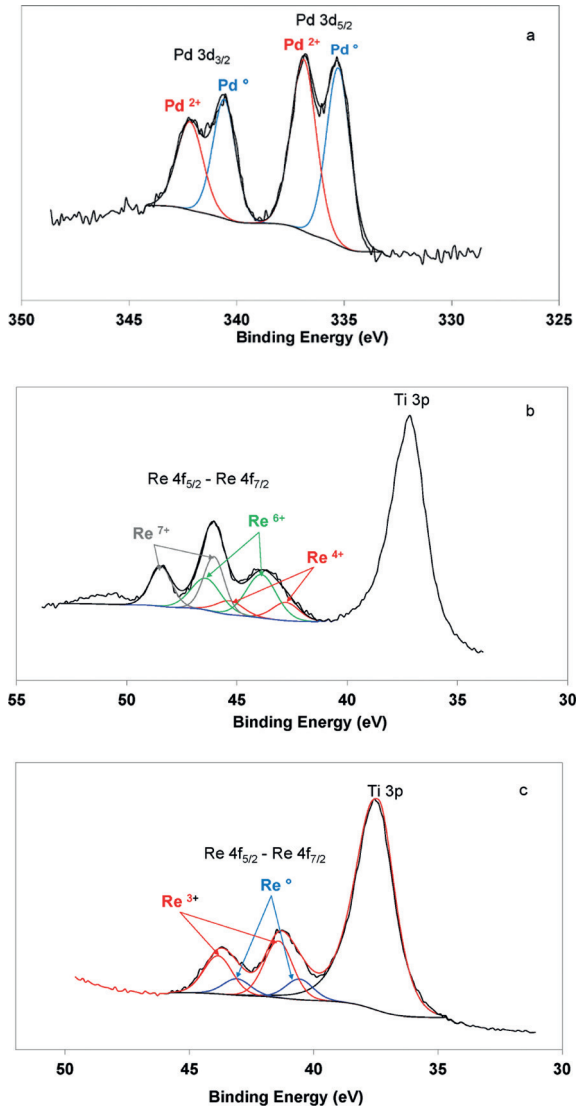

Figure 5. Curve fitting of the XPS data of 2.6 wt%Re-Pd_{KCl}/DT51-SI: a, b) Pd 3d region and Re 4f region of the solid without previous treatment and c) Re 4f region of the solid after in situ reactivation.

Exposure to air partially reoxidized the bimetallic catalysts to give ≈60% Pd^0 and ≈40% Pd^{2+} (Figure 5a; Table 1, entries 7 and 12). Additionally, no detectable fraction of Re^0 was observed in either catalyst. Three different Re BE states were shown that correspond most closely to Re^{4+}, Re^{6+}, and Re^{7+} reference standards. After curve fitting, variable surface proportions were calculated (16% Re^{4+}, 41% Re^{6+}, and 43% Re^{7+} on DT51, and 29% Re^{4+}, 24% Re^{6+}, and 47% Re^{7+} on P25; Figure 5b). Thus, as observed for the monometallic 1.9 wt%Re/P25, the Re species in the bimetallic catalysts are oxidized on exposure to air. These observations are consistent with the known oxophilic character of Re, which forms strong bonds with the oxygen atoms of the support and stabilizes rhenium oxide.[22]

The oxidation of Pd upon exposure to air was reversible as only the peak that corresponds to Pd^0 was detected in both solids at BE = 335.1 eV following a new reduction of the "as-prepared" catalysts in the XPS cell (Table 1, entries 8 and 13). In contrast, Re was difficult to reduce to the metallic state: it was again present as Re^0 and Re^{3+} with minor proportions of Re^0 of only 27 and 34% on DT51 and P25, respectively (Figure 5c; Table 1, entries 8 and 13). It is noticeable that although the 1.9 wt%$[NH_4ReO_4]_{pH1}$/P25 catalyst precursor could be reduced at 450 °C up to 89% metallic Re (Figure 4), the reduction of the bimetallic catalysts prepared by SI under the same conditions resulted in only 27–34% Re^0, regardless of if the initial state of Re was Re^{7+} in the precursors or a mixture of Re^{4+}, Re^{6+}, and Re^{7+} in the "as-prepared" solids (Table 1, entries 7 and 12). A supplementary experiment was performed in which the "as-prepared" 2.6 wt%Re-Pd/P25-SI catalyst was oxidized initially under pure O_2 (100% Re^{7+}) and then reduced at 450 °C for 3 h. Again, only 36% Re^0 could be detected in addition to 64% Re^{3+} (Table 1, entry 14). The presence of Pd limits the reduction of the oxidized Re species.

The in situ reduction of the precursor 2.6 wt%[NH_4ReO_4]-Pd on P25 and DT51 and prepared by SI gave a Re/Pd atomic ratio of 0.9 and 1.07, respectively (Table 1, entries 6 and 11). Exposure to air increased this ratio to 1.32 and 1.37, respectively (Table 1, entries 7 and 12), which suggests some migration of Re on the surface. A subsequent reactivation in H_2 at 450 °C gave ratios of 1.38 and 2.18, respectively (Table 1, entries 8 and 13), which are different from those observed after the direct reduction of the precursors.

Bimetallic Re-Pd catalysts prepared by CR

Some bimetallic catalysts prepared by the CR method were analyzed similarly after storage in air and/or after reduction in the XPS cell at 450 °C (Table 1).

The "as-prepared" 1.7 wt%Re-Pd_{Cl}/P25-CR catalyst contained Re as a mixture of Re^{4+}, Re^{6+}, and Re^{7+}; the highest oxidation state species Re^{7+} was the most abundant (63%, Table 1, entry 19). Conversely, Pd was 66% in the zero-valent state, and the remainder was Pd^{2+} (18%) and Pd^{4+} (16%). Compared to the "as-prepared" Pd monometallic parent that contained only 34% Pd^0, the presence of Re in interaction with Pd seems to limit the reoxidation of Pd. However, as in the SI-prepared catalysts, the shift of the BEs for Pd^0 and Pd^{2+} to lower energies on one part and of that of Re^{4+} and Re^{6+} to higher energies on the other part compared to the "as-prepared" 2 wt%Pd_{Cl}/P25 and 1.9 wt%Re_{pH1}/P25 was small (0.2–0.3 eV), within the experimental errors. Therefore, there is no evidence of an electronic transfer from Re to Pd in this catalyst. Although the other "as-prepared" catalysts were not characterized, one may expect the same results.

Following in situ reduction in the XPS cell, Pd was in the zero-valent state (>92%) whatever the nature of the support and the precursor salt, whereas the Re species were affected significantly by the method of preparation. If $PdCl_2$ was used as the precursor, most of the Re was present in the Re^{3+} state; the higher the amount of Re, the higher the proportion of Re^{3+} (Table 1, entries 18 and 20). However, if we start from K_2PdCl_4, the nature of the support influenced the final reduction state of Re: 74% Re^0 and 26%Re^{3+}, and 30% Re^0 and 70% Re^{3+} for 1.5 wt%Re-Pd_{KCl}/P25-CR (entry 15) and 1.9 wt%Re-Pd_{KCl}/DT51-CR (entry 9), respectively. Similar to that of the catalysts prepared by SI (except for 1.5 wt%Re-Pd_{KCl}/P25-CR), the zero-valent state of Re was absent or represented only a minor fraction and the remainder is Re^{3+}. This probably means that under reaction conditions in the aqueous phase under H_2 pressure at 160 °C most of the Re is in an oxidized state.

The surface Re/Pd, Re/Ti, and Pd/Ti compositions were calculated from the XPS analysis (Table 1). In the Pd_{Cl}/P25 series that contains Re deposited by CR, the determined atomic ratios of Re/Ti and Re/Pd increased as the loading of Re increased from 0.9 to 1.7 wt% (Table 1, entries 18 and 20), which shows that the Re loading increased at the surface. However, regardless of the treatment and the loading of Re, the Pd/Ti ratio did not change and was close to 0.036, which is the value in the parent catalyst (Table 1, entry 17). This indicates that little Re is located on the Pd, and Re was deposited at the Pd–support interface. However, the addition of Re to 1.9 wt%Pd_{KCl}/DT51 by CR decreased the Pd/Ti ratio from 0.038 to 0.027 (Table 1, entries 5 and 9). This implies that on this parent solid, Re might have been deposited on Pd by CR. However, another factor to consider for this catalyst is the experimental problem mentioned previously using this support.

TPR

The TPR of samples preoxidized under O_2 at 300 °C was performed up to 700 °C. TPR profiles of the series of catalysts prepared on Pd_{Cl}/P25 are shown in Figure 6, and the profiles for a series prepared on DT51 are shown in Figure 7. The results are summarized in Table 2.

XPS data showed that after O_2 treatment at 300 °C, Re was totally oxidized to Re^{7+}, for instance in 0.9 wt%Re-Pd_{Cl}/P25-CR, 3.6 wt%Re-Pd_{Cl}/P25-CR, and 2.7 wt%Re-Pd_{KCl}/P25-SI (not shown). Pd was oxidized to Pd^{2+} (62–80%) and Pd^{4+}.

During the reduction of the oxidized 2 wt%Pd_{Cl}/P25 solid only one H_2-consumption zone was clearly observed at room temperature (Figure 6a), which was ascribed to the reduction of oxidized Pd ($n_{H_2} = 2.7\times10^{-4}$ mol g_{cat}^{-1}; Table 2).[20] In the case of 1.9 wt%Re_{pH1}/P25, a wide consumption peak was exhibited between 230 and 340 °C, with a broad shoulder up to 450 °C (Figure 6b). According to the literature,[25,29] H_2 uptake in this temperature range is attributed to the reduction of ReO_x oxidized Re species and the reduction of the bulk titania support. Quantitative analysis reveals that the measured H_2 consumption (2.3×10^{-4} mol g_{cat}^{-1}) was lower than the theoretical consumption calculated for the complete reduction of the Re^{7+} present in the calcined solid to Re^0 (3.6×10^{-4} mol g_{cat}^{-1}) and confirmed that Re could not be reduced totally to the metal state, as shown previously by the XPS results. The reduction of *x*wt%Re-Pd_{Cl}/P25-CR bimetallic catalysts displayed a large reduction peak at a low temperature[20] (Figure 6c and d). The total amounts of H_2 consumed were higher than that exhibited by the Pd oxide in the monometallic catalyst, which suggests that contact between Re and Pd was established (Table 2). There is clearly a strong effect of Pd on the reduction temperature of Re^{7+}. The amount of H_2 consumed increased with the addition of Re (0.9 to 3.6 wt%). Furthermore, a comparison of 3.6 wt%Re-Pd_{Cl}/P25-CR and 3.5 wt%Re-Pd_{Cl}/P25-SI prepared by CR and SI, respectively, which contain very similar Re contents, evidenced a lower H_2 consumption at low temperature for the SI-prepared solid, which nevertheless remained higher than the consumption for the reduction of the Pd monometallic catalysts (Table 2). This means that a smaller fraction of Re is in contact with Pd in the SI-prepared catalyst. Accordingly, a second reduction peak was detected at higher temperatures (250–300 °C) for the bimetallic SI catalysts (Figure 6e), which could be attributed to the reduction of Re clusters isolated on the TiO_2 support.

The reduction of 2.7 wt%Re-Pd_{KCl}/P25-SI (not shown) also gave a large reduction peak that was complete at around 40 °C ($n_{H_2} = 4.5\times10^{-4}$ mol g_{cat}^{-1}). In addition, a weak consumption of 0.6×10^{-4} mol g_{cat}^{-1} around 325 °C was found for this

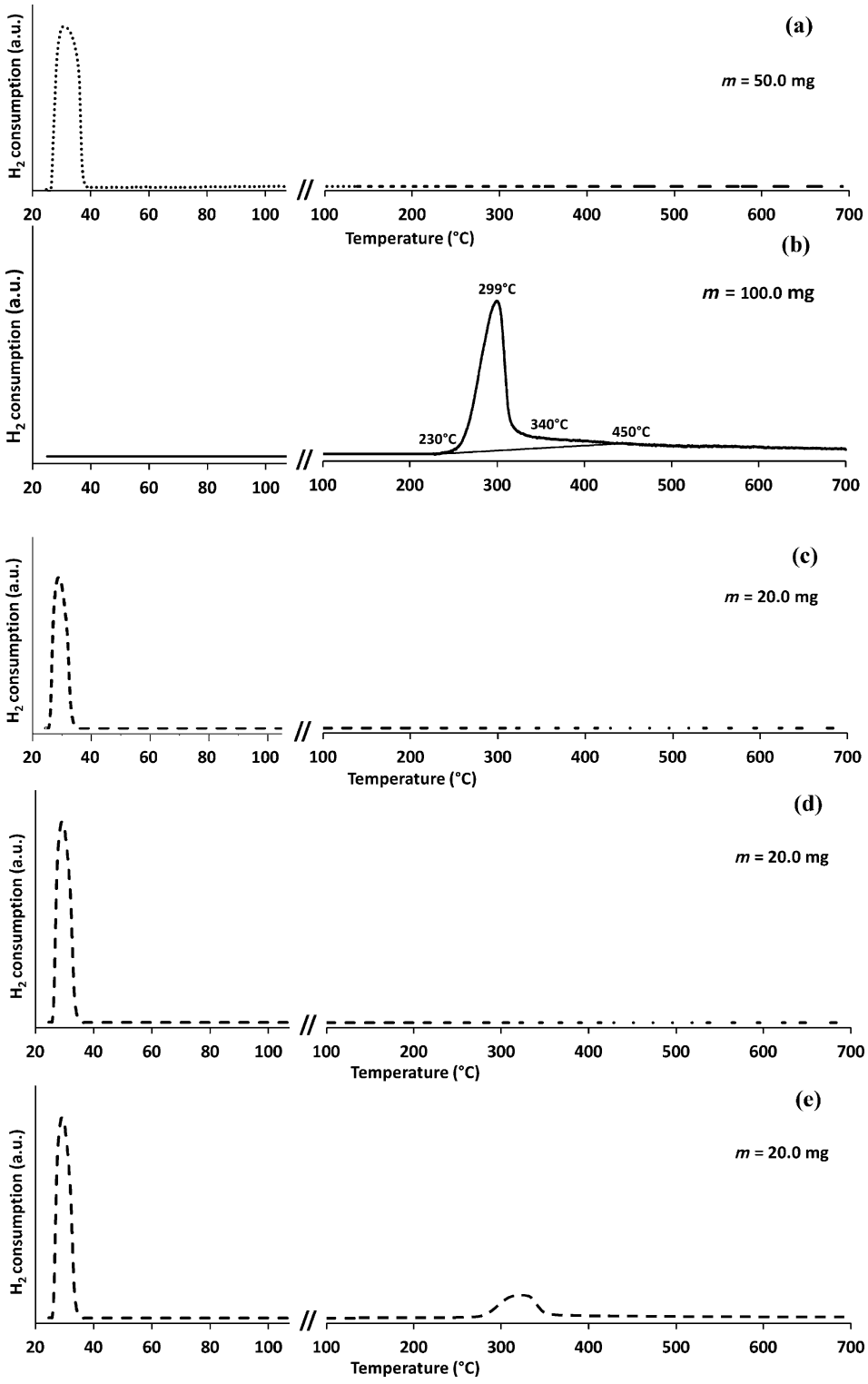

Figure 6. TPR results for the P_{Cl}/P25 series: a) 2 wtPd_{Cl}/P25, b) 1.9 wt%Re_{pH1}/P25, c) 0.5 wt%Re-Pd_{Cl}/P25-CR, d) 1.7 wt%Re-Pd_{Cl}/P25-CR, e) 3.5 wt%Re-Pd_{Cl}/P25-SI. Samples were oxidized at 300 °C before TPR analysis.

solid that could be caused by the reduction of some free isolated Re oxides or monometallic Re particles.

The catalysts prepared on DT51 presented different profiles (Figure 7). The bare support showed a consumption around 640 °C that could correspond to the reduction of the bulk TiO_2 support (Figure 7a). The reduction of oxidized Pd in 2 wt%Pd_{KCl}/DT51 was complete after 40 °C (Figure 7b). An additional consumption between 240 and 510 °C that corresponds to the reduction of the support catalyzed by Pd was also observed.[30] The TPR analysis of 1.9 wt% Re-Pd_{KCl}/DT51-CR (Figure 7c) and 3.4 wt%Re-Pd_{KCl}/DT51-SI (Figure 7d) revealed a consumption peak around 200–300 °C in addition to the consumption at room temperature. The consumption at room temperature is likely attributed to both Pd and Re in interaction with Pd. The H_2 consumptions at higher temperatures were 0.5×10^{-4} and 1.9×10^{-4} mol g^{-1}, respectively, and were ascribed to some Re that is not in contact with Pd and that may be reduced as ReO_x alone.

Hydrogen chemisorption

The bimetallic catalysts prepared by CR or SI from the three different parent Pd catalysts were characterized by hydrogen chemisorption at 70 °C. If Pd is in close interaction with Re, then its chemisorption capacity should be affected. As Re does not chemisorb hydrogen,[31] the amount of chemisorbed hydrogen will quantify the fraction of Pd atoms exposed to the surface after Re deposition in the catalysts studied.

The metallic Pd accessibility as a function of the Re loading of the bimetallic catalysts prepared by the SI or CR methods from the three monometallic parent catalysts is shown in Figure 8. The results of the parent monometallic and blank solids are given to help the interpretation. The latter were treated as for the deposition of Re but in the absence of the Re salt, that is, in acidified aqueous solution for the CR method or in neutral water for the SI method, and they are labeled blank. The effect of the addition of Re on Pd is estimated systematically by comparison with its corresponding blank sample.

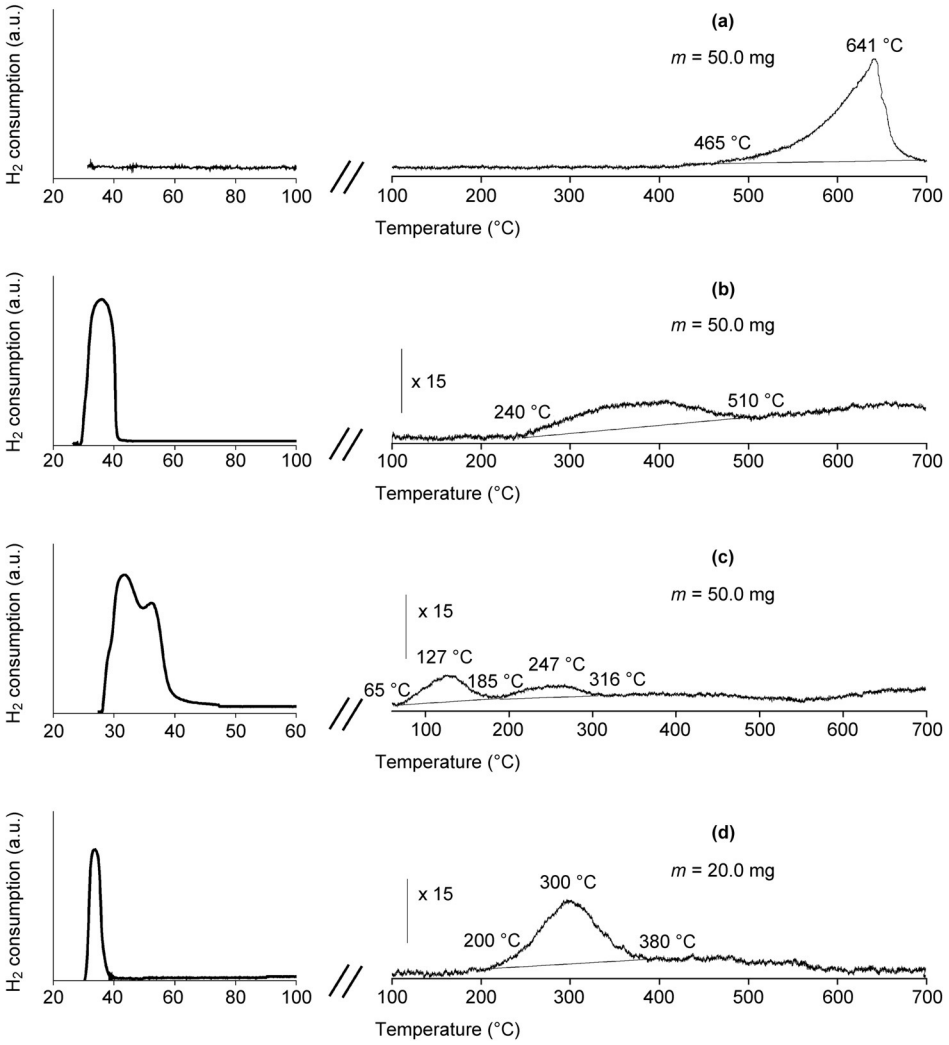

Figure 7. TPR results for the Pd_{KCl}/DT51 series: a) DT51 support, b) 2 wt%Pd_{KCl}/DT51, c) 1.9 wt%Re-Pd_{KCl}/DT51-CR, d) 3.4 wt%Re-Pd_{KCl}/DT51-SI. Samples were oxidized at 300 °C before TPR analysis.

Table 2. H_2 consumption determined from TPR profiles and XPS (after in situ oxidation at 300 °C).

Catalyst	TPR data $n_{H_2}\times10^4$ [mol g_{cat}^{-1}] Low *T*	High *T*	XPS data Pd^{4+}/Pd^{2+} [%/%]	$n_{H_2}\times10^4$ [mol g_{cat}^{-1}] for Re^{7+} reduction	OD Re[b]
2 wt%Pd_{Cl}/P25	2.7[a]	–	48/52	–	–
1.9 wt%Re_{pH1}/P25	–	2.3[a]	–	–	2.55
0.5 wt%Re-Pd_{Cl}/P25-CR	3.2	–	38/62[c]	0.2	5.5
0.9 wt%Re-Pd_{Cl}/P25-CR	3.8[a]	–	31/69	0.9	3.03
1.7 wt%Re-Pd_{Cl}/P25-CR	4.1	–	25/75[c]	1.6	3.50
2.4 wt%Re-Pd_{Cl}/P25-CR	4.2	–	22/78[c]	1.8	4.2
3.6 wt%Re-Pd_{Cl}/P25-CR	5.1	–	20/80	2.8	4.1
3.5 wt%Re-Pd_{Cl}/P25-SI	4.1[a]	1.5[a]	–	–	–
2.7 wt%Re-Pd_{KCl}/P25-SI	4.5	0.6	20/80	2.3	3.82
2 wt%Pd_{KCl}/DT51	3.1	0.8	–	–	–
1.9 wt%Re-Pd_{KCl}/DT51-CR	3.8	0.5	–	–	–
3.4 wt%Re-Pd_{KCl}/DT51-SI	3.6	1.9	–	–	–

[a] Results in Ref. [20]. [b] Average oxidation valence OD = 7−*x*, calculated from $Re^{7+}+x/2\,H_2\rightarrow Re^{7-x}+x\,H^+$, with $x=2\,n_{H_2}/n_{Re^{7+}}$. [c] Calculated assuming a linear correlation as a function of wt%Re.

The monometallic Pd catalysts showed different abilities to withstand sintering during the CR or SI treatment, depending on the preparation method. The accessibility to hydrogen of blank 2 wt%Pd_{KCl}/P25-CR and -SI solids obtained after the treatment of 2 wt%Pd_{KCl}/P25 in an acidic solution under H_2 or in neutral water, respectively, did not change much (Figure 8a and b). The values were 15, 18, and 15%, for the parent and the CR- and SI-treated samples, respectively. Similarly, although the dispersion of 2 wt%Pd_{KCl}/DT51 was higher than that on Pd_{KCl}/P25, the blank treatments did not modify the metallic accessibility, and the values were 27, 30, and 23%, for the parent and the CR- and SI-treated solids, respectively (Figure 8c and d). In contrast, as described previously,[20] the CR blank protocol applied to 2 wt%Pd_{Cl}/P25 resulted in a sintering of the Pd particles with a significant decrease of the metallic accessibility from 33 to 17% (Figure 8e). However, exposure of this parent catalyst to the SI neutral solution under ambient air only slightly decreased the accessibility from 33 to 26% (Figure 8f). The sintering of the metallic particles in acidic medium is in agreement with results in the literature on the preparation of such catalysts.[32–34]

The reason why the blank treatment by the CR protocol of 2 wt%Pd_{Cl}/P25 involved a significant sintering of the metallic particles compared with 2 wt%Pd_{KCl}/P25 may result from different factors. The initial Pd dispersion was much higher in the first system, which therefore, may be more prone to sintering. However, a stronger metal–support interaction, linked to the impregnation conditions, may explain the high stability of the catalysts prepared from K_2PdCl_4 solutions.

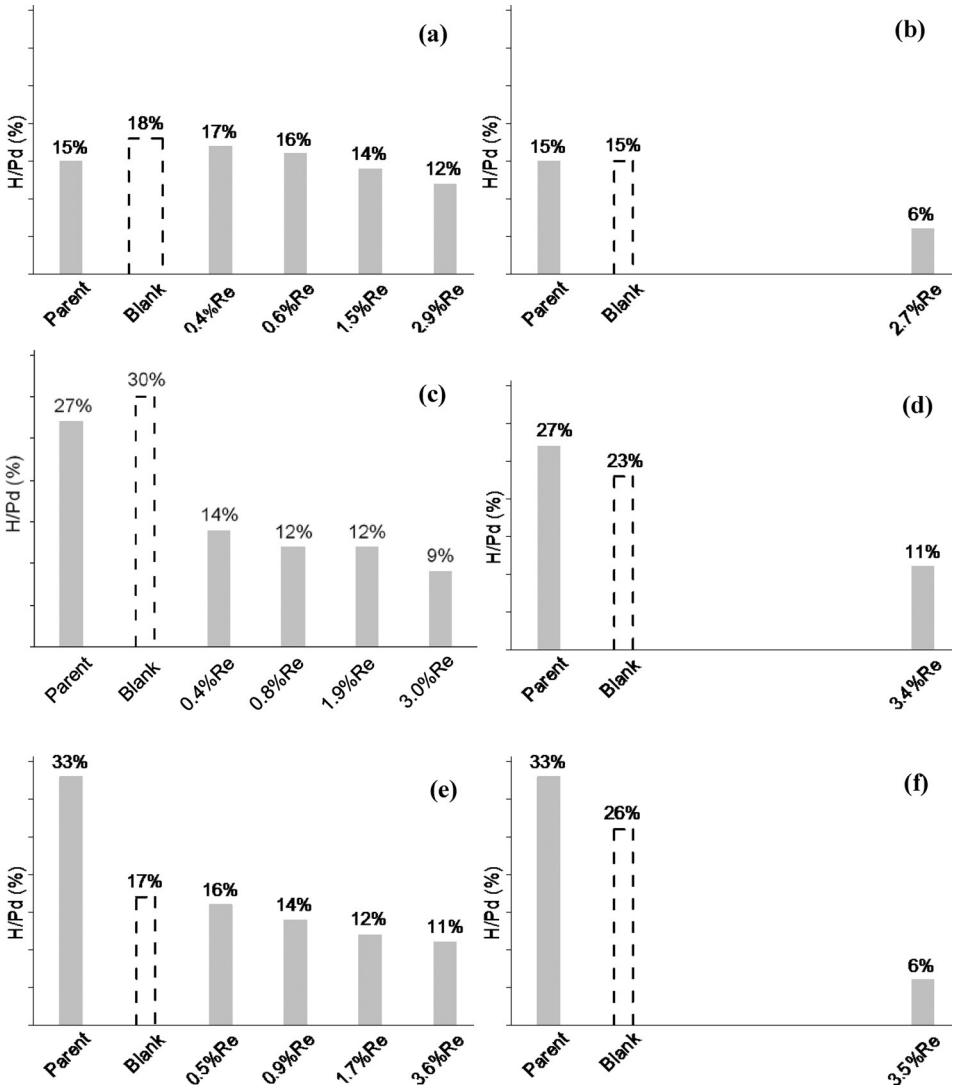

Figure 8. Pd accessibility (H/Pd) of bimetallic catalysts prepared by CR (left) and SI (right) by the addition of Re onto: a, b) Pd_{KCl}/P25, c, d) Pd_{KCl}/DT51, and e, f) Pd_{Cl}/P25.

This second hypothesis is confirmed by the stability of the relatively well dispersed Pd metallic phase in Pd_{KCl}/DT51 also obtained by deposition–precipitation in alkaline medium.

The H/M ratio decreased with the addition of Re compared to the blank treated parent catalysts for all series of catalysts (Figure 8), which tends to demonstrate the presence of Re deposited on the Pd surface. However, this covering was more or less important depending on the preparation method and on the support used, which is discussed below.

Pd_{KCl}/P25

On 2 wt%Pd_{KCl}/P25, the accessibility to hydrogen decreased gradually from 18 (blank) to 16, 14, and 12% as Re loadings by CR increased from 0 to 0.6, 1.5, and 2.9 wt%, respectively (Figure 8a). As the comparison was performed with the corresponding blank sample, this effect should not be attributed to a lower metal dispersion but to some coverage of the Pd surface by Re. However, the decrease was not very significant even after a 2.9 wt% Re loading. Furthermore, if we consider an initial accessibility of 18%, we can calculate that approximately 0.6 wt% Re loading corresponds to a theoretical monolayer covering of Pd. It is then likely that the available Pd sites for direct Re–Pd bonding become rapidly saturated, and the Re moieties were not only deposited on the initial Pd surface of 2 wt%Pd_{KCl}/P25 but Re could also have been deposited adjacent to Pd particles at the Pd–TiO_2 interface, and/or even as clusters or agglomerates on particular sites. The presence of Re on the support cannot be excluded. Nevertheless, a high fraction of Re loading on the support that would not be in contact with Pd could certainly be excluded as the preparation of a Re catalyst with a nominal Re loading of 4 wt% by the CR method on the bare P25 support (which contains no Pd) led only to a 0.3 wt% Re deposit on the solid. Therefore, on the bimetallic catalyst, it may be considered that Re was deposited marginally on the support without interaction with Pd but mainly deposited at the Pd–support interface in close vicinity to Pd.

In contrast to the CR protocol, the loading of 2.7 wt% Re by the SI method on the same parent 2 wt%Pd_{KCl}/P25 (Figure 8b) led to a significant decrease of the H/Pd ratio from 15 to 6%. As the blank Pd_{KCl}/P25-CR and -SI solids showed similar dispersions (18 and 15%, respectively), a comparison with results for the 2.9 wt%Re-Pd_{KCl}/P25-CR catalyst suggests that the covering of the Pd surface by the SI method is more efficient than that by the CR deposition. This is surprising if we consider the theoretical metal deposition by CR on the Pd surface.

Pd_{KCl}/DT51

The results of H_2 chemisorption for the bimetallic catalysts prepared from the 2 wt%Pd_{KCl}/DT51 parent catalyst are illustrated in Figure 8c and d. The variation of H/Pd for this series of CR catalysts was different from the CR series prepared from the 2 wt%Pd_{KCl}/P25 catalyst. This time, even after the deposition of only 0.4 or 0.8 wt% Re by CR, the Pd accessibility decreased considerably from 30 to 14 and 12%, respectively (Figure 8c). It then decreased slowly to 9% with further loading of Re up

to 3.0 wt%. The crystal structure of the support used might be an important parameter. Although P25 is a mixture of rutile and anatase phases with a specific surface area of 50 $m^2 g^{-1}$, DT51 is constituted of anatase only and presents a specific area of 88 $m^2 g^{-1}$. It cannot be excluded that the rutile phase favors the selective deposition of Re at the Pd–support interface. This may also result from the experimental problems encountered during the preparation using the CR protocol on the DT51-supported catalyst mentioned above, that is, the plugging of the frit and an inhomogeneous H_2 flow, which could lead to a different deposition. Finally, the loading of 3.4 wt% Re by SI also decreased the metallic accessibility significantly, which decreased to 11% (Figure 8d). This means that the coverage of Pd by the deposition of 3.4 wt% Re by SI on Pd_{KCl}/DT51 was less important than that of 2.7 wt% Re by SI on Pd_{KCl}/P25. This difference might be because of the different specific area of the supports. Notably, an approximately 3 wt% Re loading by both methods on this 2 wt%Pd_{KCl}/DT51 parent catalyst gave catalytic systems that present very close H_2 accessibility, that is, ≈10%.

Pd_{Cl}/P25

As for the series prepared from the P25 support, the deposition of increasing amounts of Re by CR on Pd_{Cl}/P25 only slightly decreased the H/M ratio compared to that of the blank treated solid: 16, 14, 12, and 11% following the addition of 0.5, 0.9, 1.7, and 3.6 wt%, compared to 17%, respectively (Figure 8e), which evidences the deposition of Re on Pd. However, as observed for Pd_{KCl}/P25, the H/Pd ratio remained very close to the value of the blank (17%) in particular at low Re loadings. A limited sintering of the Pd particles caused by the CR protocol (immersion of the catalyst in an acidic aqueous solution of pH 1 under H_2 flow) in the presence of Re in solution could be an explanation. Indeed, on Ge-Rh/SiO_2 catalysts prepared by the same CR protocol, the sintering process was less important if compared with the blank treated Rh/SiO_2 solid.[35] This behavior was explained by the consumption of adsorbed activated hydrogen on the surface of the metallic Rh surface during the reduction of the Re salt. Indeed, adsorbed hydrogen favors the sintering of metallic particles in the aqueous phase.[34] Then, at higher loadings of 3.6 wt% Re by the CR protocol, the accessibility remained constant at ≈11%. This suggests that Re does not deposit uniformly on the Pd surface but may occur at the particle–support interface and/or as aggregates close to Pd as suggested above for the Re-Pd_{KCl}/P25-CR catalysts, which thus leaves a non-negligible accessible Pd metallic surface. Finally, the deposition of 3.5 wt% Re on Pd_{Cl}/P25 by SI occurred on the entire available Pd surface and on the support, as demonstrated by the dramatic decrease of the hydrogen accessibility from 26 to 6% (Figure 8f).

Cyclohexane dehydrogenation

The catalytic activity for cyclohexane dehydrogenation at 270 °C was used as a probe to investigate the exposed metal surface as this reaction is known to be structure insensitive, that is, the activity should be approximately proportional to the amount of surface Pd atoms and not influenced by the presence of Re.[36–39] The deviation from linearity can be caused by the differences in the electron density of Pd, which may be affected by the addition of Re. The participation of Re on the reaction should be negligible under the reaction conditions chosen.[40]

The TOF in cyclohexane dehydrogenation calculated from the specific reaction rates based on the Pd dispersion values (H/M) are illustrated in Figure 9 (values given for 0 wt% Re correspond to those of blank samples).

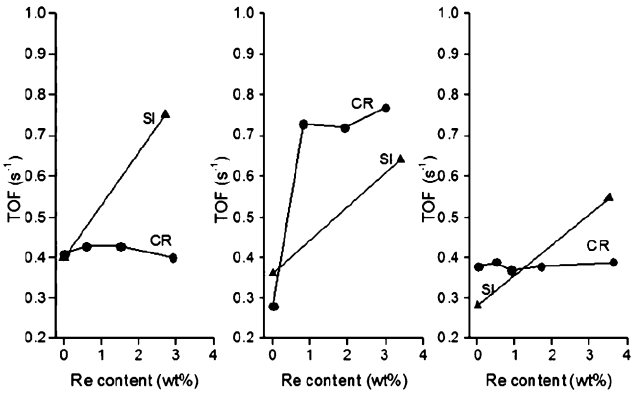

Figure 9. TOF values for cyclohexane dehydrogenation with a) *x*wt%Re-Pd_{KCl}/P25, b) *x*wt%Re-Pd_{KCl}/DT51, and c) *x*wt%Re-Pd_{Cl}/P25.

The TOF values for the bimetallic catalysts supported on P25 (prepared from 2 wt%Pd_{KCl}/P25 or 2 wt%Pd_{Cl}/P25) that contain Re deposited by CR were around 0.4 s^{-1}, which is very close to that of blank Pd_{KCl}/P25-CR and blank Pd_{Cl}/P25-CR (0.41 and 0.38 s^{-1}, respectively). This results from the absence of electronic modifications of Pd in catalysts prepared under CR conditions on P25, whatever the preparation method of the monometallic catalyst. In contrast, the bimetallic catalysts that also contain Re deposited on DT51 although prepared by CR, showed a significant increase of the TOF to ≈0.7 s^{-1}, compared with 0.28 s^{-1} for the blank CR solid. Moreover, the implementation of the SI protocol led to bimetallic catalysts with high TOF values whatever the support (0.75, 0.64, and 0.55 s^{-1} after the loading of 2.7, 3.4, and 3.5 wt% Re on Pd_{KCl}/P25, Pd_{KCl}/DT51, and Pd_{Cl}/P25, respectively).

To explain these differences, in a first step, it was verified whether a supported monometallic Re catalyst was able to participate to the reaction. The 1.9 wt%Re_{pH1}/P25 solid after in situ reactivation at 450 °C gave a low but non-negligible specific activity of 0.84 mol h^{-1} g_{Re}^{-1} (compared to 1.5–3.5 mol h^{-1} g_{Pd}^{-1} for the Pd-based catalysts). It was demonstrated by XPS that this solid contained 15% Re^0 and 85% Re^{3+} at the surface of the catalyst (Table 1, entry 3). This would suggest

that Re in the zero-valent state could effectively catalyze the reaction.

In a second step, we considered the reduction degree of Re to the zero-valent state in the bimetallic catalysts as determined by XPS after in situ reduction at 450 °C. In all reduced samples, no modification of the electronic state of Pd could be evidenced by XPS on the addition of Re. As shown previously, depending on the support, the Pd precursor, and the deposition method, the reduced bimetallic Re-Pd catalysts examined contained different proportions of Re^0 and Re^{3+} (Table 1). However, until now we have not been able to establish a correlation between the method of preparation and the resulting oxidation degree of Re (Re deposited on Pd_{KCl}/DT51 by SI (2.6 wt%) or CR (1.9 wt%), on Pd_{KCl}/P25 by SI (2.7 wt%) was present as ≈30% Re^0 and 70% Re^{3+}). Re introduced on 1.5 wt%Re-Pd_{KCl}/P25 by CR was more reduced (74% Re^0). However, the 0.9 wt% Re and 1.7 wt% Re catalysts prepared by CR on Pd_{Cl}/P25 contained mainly or only 100% Re^{3+}. Nevertheless, it is noticeable that catalysts that contain Re^0 (≈30%; except 1.5 wt%Re-Pd_{KCl}/P25-CR, which surprisingly contained 75% Re^0) resulted in a significant increase in TOF (0.6–0.7 s^{-1}), which would again suggest a possible contribution to the dehydrogenation reaction of metallic Re in bimetallic catalysts. Furthermore, if the activity of catalysts that contain Re^0 is proportional to the amount of metallic Re and if we consider the activity of 1.9 wt%Re_{pH1}/P25 (15% Re^0) of 0.84 mol h^{-1} g_{Re}^{-1}, the activity attributed to Pd in, for example, 1.9 wt%Re-Pd_{KCl}/DT51-CR (30% Re^0) should be 1.22 mol h^{-1} g_{Pd}^{-1}, which would result in a TOF of 0.3 s^{-1} for Pd^0. This value is very close to the TOF of the monometallic catalyst (0.28 s^{-1}). These results suggest that the higher activity observed for some bimetallic catalysts in the dehydrogenation reaction is just the sum of the contributions of both metallic Pd and Re. The absence of change of the TOF in the absence of Re^0 shows that the addition of Re does not modify the electronic state of Pd.

In contrast, there are some data in the literature that demonstrate a strong interaction in Re-Pd catalysts[17,41] and other Re-based bimetallic solids. A considerable interaction was also concluded for reduced Re-Pd/Al_2O_3 catalysts prepared by SI.[42] High-resolution transmission electron microscopy (HR-TEM) images of Re-2 wt%Pd/C (Re/Pd molar ratio 0.6) prepared by incipient wetness impregnation, drying, and reduction at 300 °C showed Pd particles and some alloy bimetallic particles with a lattice expansion associated with the incorporation of Re into the Pd lattice.[17] The formation of surface bimetallic clusters on the surface of TiO_2 was demonstrated in Pt-Re/TiO_2 and Pd-Re/TiO_2.[43] The addition of Re to Pt/C resulted in a decrease in the electron density of both Pt and Re as shown by the shift to higher energies with increasing Re content in the bimetallic catalysts.[44]

Catalytic performance

GBL and BDO are the main products of SUC hydrogenation. THF, propanol, and butanol are produced as minor byproducts (THF < 10%; propanol, butanol < 2%).

A comparison between the behavior of the catalysts for SUC hydrogenation has been reported previously.[19] Typical concentration profiles observed for SUC hydrogenation in the presence of a Pd and a ReO_x-Pd catalyst are shown in Figure S8. The catalytic results are shown schematically in Figure 10.

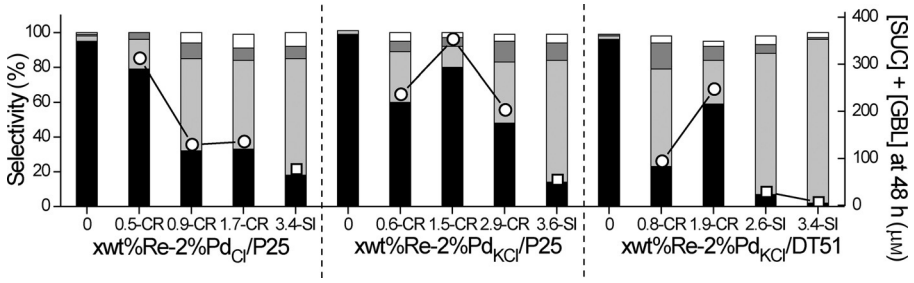

Figure 10. Effect of various amounts of Re added to Pd on SUC hydrogenation. Left: selectivity to GBL (black), BDO (light grey), THF (dark grey), others (white); right: unconverted (GBL+SUC) concentration after 48 h (open square or circle). Reaction conditions: SUC (6 g) in water (114 g; 0.43 mol L^{-1}), P_{H_2} = 150 bar, T = 160 °C, 0.5 g catalyst, t = 48 h.

Globally, a positive effect on the reaction rate of SUC to GBL was usually observed as the amount of Re increased, though the optimal amount using the CR method passed through a maximum. Indeed, the time required to observe 50% conversion of SUC to GBL in the presence of the different catalysts was as follows: Pd_{Cl}/P25, 8 h; 0.5 wt%Re-Pd_{Cl}/P25-CR, 8 h; 0.9 wt%Re-Pd_{Cl}/P25-CR, 3 h; and 1.7 wt%Re-Pd_{Cl}/P25-CR, 5 h for the Pd_{Cl}/P25 series; Pd_{KCl}/P25, 29 h; 0.6 wt%Re-Pd_{KCl}/P25-CR, 8 h; 1.5 wt%Re-Pd_{KCl}/P25-CR, 15 h; and 2.9 wt%Re-Pd_{KCl}/P25-CR, 12 h for the Pd_{KCl}/P25 series; Pd_{KCl}/DT51, 12 h; 0.8 wt%Re-Pd_{KCl}/DT51-CR, 3 h; and 1.9 wt%Re-Pd_{KCl}/DT51-CR, 12 h for the Pd_{KCl}/DT51 series. The time for the SI-prepared catalysts was in the range 2.5–3 h except for 3.4 wt%Re-Pd_{Cl}/P25-SI (7 h). The rate of GBL conversion to BDO is reflected by the final selectivity as described in Figure 10. The most important point is the remarkable effect on the selectivity to BDO.

Although the selectivity to BDO was almost null using Pd/TiO_2 catalysts, promotion by Re made the ring-opening and hydrogenation of the GBL intermediate to BDO possible. However, the selectivity was strongly affected by the support, the preparation method of the Pd catalyst, and the Re deposition procedure. The optimum amount of Re promoter required by the CR protocol (0.6–0.9 wt%) to allow high selectivities to BDO was lower than that for the SI protocol (3–4 wt%). An increase in the loading of Re by CR above this optimum value has little effect on catalyst selectivity, although there was a gen-

eral trend of decreasing conversion at high loadings. If we used the SI protocol, a high Re content, high activity, and high selectivity to BDO were achieved.

Discussion

Distribution of Re species in the catalysts

Reducibility of Re in the monometallic Re catalyst

The reducibility of Re in monometallic samples must be clarified as a fraction of Re may be deposited on the support during bimetallic preparation. The TPR of the 1.9 wt%Re_{pH1}/P25 monometallic catalyst revealed a large peak of H_2 consumption at ≈330 °C attributed to the reduction of various oxidized Re species (Figure 6). Quantitative analysis by XPS showed that the solid after reduction is still composed of a complex mixture of surface species. Only 15% Re^0 was identified after the rereduction of the "as-prepared" solid on P25 (Figure 4c, Table 1, entry 3), compared to 89% Re^0 following the reduction of the precursor (Figure 4a, Table 1, entry 1), which suggests that the reduction of a mixture of partly oxidized dispersed Re species is more difficult than the direct reduction of Re^{7+} to Re^0. The finding that a fraction of Re is not completely reduced to the metallic state even after reduction at 450 °C is consistent with the results of the reducibility of rhenium oxide in supported monometallic catalysts prepared from NH_4ReO_4, which has been debated in the literature, mainly on alumina.[25] Re is oxophilic and may bond strongly to metal oxide surfaces. The reducibility is a function of the Re loading (the interaction might be very strong at low concentration and decrease with the increasing coverage of Re), the calcination temperature, the adsorbed moisture, and the strength of the interaction of the Re clusters with the O atoms of the support (which decreases in the order $Al_2O_3 > SiO_2 \sim ZrO_2 > TiO_2$).[22,25,29,45–47] Bare et al. used several techniques to show that Re is present as a mixture of species (unreduced Re^{7+} species, small clusters, and isolated atoms) after the reduction of 0.7 wt%Re/γ-Al_2O_3.[25] It was also suggested by extended X-ray absorption fine structure analysis (EXAFS) that a Re/Al_2O_3 catalyst after reduction at 400 °C contained a fraction of rhenium oxide in addition to highly dispersed metallic particles on the support surface.[45]

The reason why the Re species were more difficult to reduce to the metallic state after exposure to air may be explained by the weak interaction of Re with the support. It is possible that upon exposure to ambient air these Re particles redisperse to more highly dispersed surface rhenium oxides that could interact more strongly with the support and be more resistant to complete reduction. The metal oxidation state of Pt-Re supported on Al_2O_3 and TiO_2 was determined by in situ XANES in solvents in autoclave reactors at 120 °C under 10 bar H_2 pressure.[41] It was harder to reduce Re on TiO_2 than on alumina. TiO_2 seemed to have a fraction of Re not associated with Pt, which is different from that on Al_2O_3. It was proposed that some of the Re was not in contact with Pt, which makes it harder to reduce. Additionally, the strong interaction between ReO_x and TiO_2 might play a role.

Structure and interaction between Pd and Re in the bimetallic catalysts

The data obtained by the different techniques with regard to the structure of the bimetallic catalysts and the nature of the interaction of the two metals are sometimes inconsistent, however, the balance is in favor of the presence of some Pd–Re interactions without significant electron modifications of Pd and Re sites. We tried to highlight the differences, if any, when we compared the different catalysts.

According to the results of H_2 chemisorption, the deposition of Re onto the Pd catalyst decreased the hydrogen accessibility of Pd, although significant differences were observed. If we used the CR protocol, the decrease was moderate, which indicates a very low coverage of the Pd surface with ReO_x species. In contrast, the exposed Pd surface was modified significantly using the SI protocol, which suggests a higher coverage of Re on the Pd surface for a given loading of Re.

It was difficult to detect Re particles by TEM because of the high dispersion of Re species. Nevertheless, the EDX analysis confirmed the presence of both Pd and Re in small or large analysis zones. However, STEM in dark-field mode at high resolution and the corresponding analysis was able to image the Re nanoclusters (< 0.7 nm) located everywhere on the Pd particles in the bimetallic catalyst and on the support. The deposition of Re located specifically on Pd could not be visualized. The presence of Re clusters all over the catalyst is consistent with the low Re coverage of the Pd surface of Pd_{KCl}/P25 with increasing loadings of Re, even at 1.5 wt% Re addition (Figure 8).

In the impregnated materials and after oxidation, Re was present as Re^{7+} only (XPS data). TPR profiles of preoxidized samples showed that the H_2 consumption at low temperature in the bimetallic catalysts was higher than that in the parent catalysts, which suggests that some of the Re oxide might be reduced at lower temperatures compared with the monometallic Re catalyst, if it interacts with Pd or in close vicinity of Pd. In the Pd_{Cl}/P25 catalyst series, the amount of H_2 consumed increased with the amount of Re deposited by CR from 0.5 to 3.6 wt% (Table 2). However, even after reduction at 450 °C, the complete reduction of Re to the zero-valent state was not observed by XPS, which signifies that even if Re reduction was facilitated by contact with Pd, all of the Re was not reduced to the metal.

In the XPS spectra of Pd and Re in the bimetallic catalysts measured in an in situ cell, there was no clear indication that the addition of Re caused a shift of the BEs of reference materials, which excludes strong electronic perturbations. These results suggest that the vast majority of Re is located preferentially in contact with Pd but without electronic interaction. The sites are thought to consist of metallic Pd surface sites with neighboring Re atoms. In the XPS spectra there is a trend that the distribution of Re species shifts to more oxidized species as the content of Re increases. This is shown, for instance, in the comparison of 0.9 wt%Re-Pd_{Cl}/P25-CR and 1.7 wt%Re-Pd_{Cl}/P25-CR (Table 1, entries 18 and 20).

More information can be gained if we determine the H_2 consumption during TPR, which may be assigned to the reduction of oxidized Re in addition to the reduction of oxidized Pd. To calculate these values, the oxidation degree of Pd and Re before TPR was determined by XPS after O_2 pretreatment at 300 °C in the XPS cell (which mimics the oxidation treatment before the TPR experiments); Re was in its highest oxidation state of +7, whereas Pd was present as Pd^{2+} and Pd^{4+}. The Pd^{4+}/Pd^{2+} distribution of 48/52% in Pd_{Cl}/P25 changed to 31/69% and 20/80% on the addition of 0.9 and 3.6 wt% Re by CR, respectively (Table 2). This distribution was 20/80% in 2.7 wt%Re-PdKCl/P25-SI. Re in contact with Pd seems to prevent Pd from strong oxidation, as mentioned above.

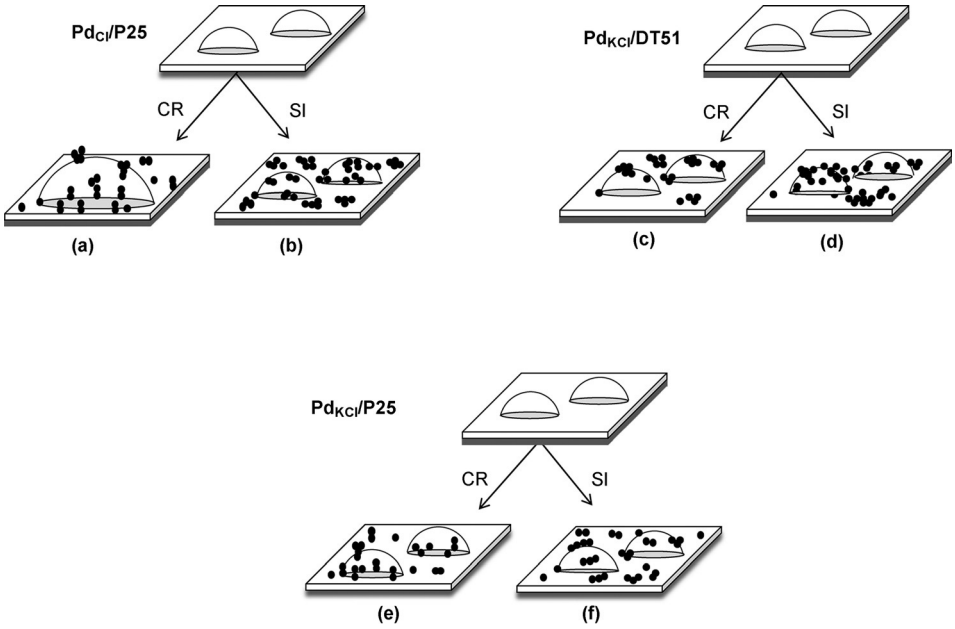

Figure 11. Schematic representation of the ReO_x-Pd bimetallic catalysts.

The calculated H_2 consumptions for the reduction of Re^{7+} characterized both by TPR and XPS are reported in Table 2. A Re average oxidation valence (OD) was deduced from these values and is also reported in Table 2. The average OD of Re in the CR- and SI-prepared bimetallic catalysts evolved between 3.0 and 5.5. The 1.9 wt%Re_{pH1}/P25 reduced catalyst showed a lower OD (2.5) than the bimetallic catalysts. The CR-prepared bimetallic catalyst with the lowest Re content (0.5 wt%) displayed the highest OD value (5.5), which suggests that Re species in a highly dispersed state (probably in an atomic form) are very difficult to reduce. For the other CR-prepared bimetallic catalysts of the series, the OD tends to increase with the Re addition on Pd_{Cl}/P25. This means that less Re comes into direct contact with Pd as the Re loading increases. This hypothesis is in agreement with the hydrogen accessibility, which reached a plateau at 10% in this series. As the Re loading increases, the Re species are reduced, although to a higher oxidation degree if they are deposited close to Pd, however, without decreasing the Pd accessibility; it will also be deposited as ReO_x nanoclusters isolated on the support as observed clearly by HAADSTEM on 1.5 wt%Re-Pd_{KCl}/P25 (Figure 3). The reduction of these ReO_x nanoclusters on the support was not detected by TPR, which signifies that they may interact strongly with the support. In contrast, in the catalysts prepared using the SI protocol, the reduction of the ReO_x clusters isolated on the support was detected by TPR, which indicates that these aggregates are larger and do not interact with the support.

Schematic representation of bimetallic catalysts

We can now propose a structural model for the location of Re on the catalyst surface that is consistent with the characterization data and explains the performance trends observed with the different catalysts (Figure 11). Alternative locations were considered: (i) Re is deposited on the existing Pd crystallites, (ii) Re is in the immediate vicinity of the existing Pd, (iii) Re is on the support surface. If Re did not contribute to the decrease of Pd accessibility, this could suggest that the Re deposits as multilayer structure or is located on the support. The distribution of reduced Re surface species must also be influenced strongly by the Re content.

First, let us consider the CR method, which relies on the formation of Pd-H_{ads}, known to be a strong reductant, during the bimetallic preparation. At the beginning of the deposition of Re on Pd_{Cl}/P25 and Pd_{KCl}/P25 (Figure 11a and e), the adsorbed atomic hydrogen on Pd acts to reduce ReO_4^- to ReO_x species. Notably, the Pd particles were shown to grow during the deposition of Re by CR on Pd_{Cl}/P25. This initial fraction of Re should be strongly immobilized. The stoichiometry of the reaction of the deposition of these Re species is not demonstrated, but one may expect low valences. However, XPS analysis indicated that most of the time, only a minor part of Re was reduced fully to the metallic state. These highly reduced Re surface species might be more resistant to reoxidation by exposure to oxygen. As the Pd accessibility (as measured by chemisorption) decreased only moderately with increasing amounts of Re by CR in both series (Figure 8a and e) and as Re is shown to be reduced in contact with Pd (as measured by TPR), we propose that the deposition occurs of course on the Pd surface because of the oriented method but also mainly at the interface of the Pd particles and the support. Moreover, we suggest that incremental deposition on the Pd particles occurs as clusters by stacking on the initially deposited ReO_x species rather than as isolated species, which would then take place

without a significant decrease of the Pd accessibility. These additional Re layers should be less reduced than those closest to the Pd nanoparticles. This situation would be somewhat analogous to that described by Koso et al.[48,49] who examined MoO_x-Rh and ReO_x-Rh/SiO_2 in detail. Although the amounts of CO adsorption decreased similarly as a function of the amount of Mo or Re, EXAFS indicated that Mo was adsorbed as isolated MoO_x, whereas Re was deposited as ReO_x clusters. As a result, the optimum promoter/Rh ratio for activity in tetrahydrofurfuryl alcohol was not the same. With a further increase of the amount of additive, ReO_x clusters might increase or be deposited all over the TiO_2 support and yet leave some non-negligible Pd accessibility according to HAAD-STEM and chemisorption studies. All of the added Re will not promote the Pd catalyst further, and the selectivity to BDO will decrease with too high a loading (Figure 10).

The tendency followed by the catalysts synthesized by the CR deposition method on Pd_{KCl}/DT51 was different from the case of the two previous solids (Figure 11 c). Even a deposition as low as 0.4 wt% Re decreased the Pd accessibility by a factor of two (Figure 8 c), which suggests that the Pd surface was very efficiently covered by Re species. Increasing amounts of Re were added in a way that scarcely modified the available Pd surface to chemisorption, either as aggregates on the metal or as clusters on the support. However, these samples should be treated with some caution as one must be aware of the experimental problems encountered during the synthesis.

In the case of the SI protocol applied to the three monometallic catalysts (Figure 11 b, d, and f), the important point is that the Pd accessibility decreased more significantly for ≈3–3.5 wt% Re than in the case of the materials synthesized by the CR protocol. This could signify that modification of Pd by the Re species occurs differently, for instance as ReO_x clusters that cover a relatively large area of Pd atoms. Even at low loadings, Re is deposited randomly on the Pd particles and on the support. We propose that Re is deposited on Pd as island clusters rather than as multilayer clusters, which was the case for the oriented CR method. Consequently, the Pd accessibility will decrease more rapidly and, as shown by the catalytic tests (Figure 10), a higher amount of Re is needed to obtain high yields of BDO. The ReO_x on the support might be a larger amount and might not interact with the support, which explains that some areas are reduced at a higher temperature than the smaller clusters obtained by CR as observed by TPR (Figure 6).

Additional studies using EXAFS and CO chemisorption could help to gain a better understanding of the local structure and the degree of coverage of Pd with ReO_x species, as shown by Tomishige et al. for ReO_x-Pt and ReO_x-Ir catalysts.[50,51]

pletely reduced to the metal state and significant amounts of partially oxidized Re in the range Re^{3+}–Re^{7+} are present. This may be indicative of an active role of oxidized Re during SUC hydrogenation during the GBL reduction.

Supported bimetallic catalysts composed of a reducible noble metal (Pt, Ir, Rh, Pd) and an oxophilic metal (such as Re) have been described for the conversion of biomass-derived feedstock, the aqueous-phase reforming of biomass-derived oxygenates,[52,53] secondary C–O bonds hydrogenolysis in a broad range of polyols including glycerol[54–58] and cyclic ethers,[48,49,56,59,60] and for amide,[61] acid,[62] and amino acid[63] hydrogenation. As described in recent publications, Re promotion may generate a bifunctional catalyst that possesses both metal and Brønsted acid sites. The presence of acid sites on ReO_x-promoted metallic catalysts was revealed by NH_3-TPD profiles.[53,57] NH_3-TPD measurements also revealed that the acid site density increased with the Re loading of Pt-ReO_x catalysts.[64] Such an acid–metal bifunctional mechanism has been proposed for the hydrogenation of tertiary amides[61] or (hydroxymethyl)tetrahydrofuran derivatives over bimetallic catalysts composed of a noble metal (Rh or Pt) and Re promoter.[59,65] Under hydrothermal conditions, hydroxylated Re surface species are able to activate ring-opening by deprotonation and interaction with the reactant molecules with proton donation followed by metal-catalyzed hydrogenation.

This type of mechanism might be considered for our system (Scheme 2). The conversion of SUC to BDO occurs in two steps (Figure S8). SUC is converted to GBL, which is subsequently transformed to BDO and THF after nearly complete conversion of GBL. Significant hydrogenolysis of GBL was only observed in the presence of the bimetallic catalysts, which highlights the essential role of Re in this step. The activation of GBL on protonated Re bound to Pd may occur through both the oxygen in the cycle and the carbonyl group to yield an ester intermediate. The ring-opening of this cycle then takes place in water, and further hydrogenation over Pd will yield BDO. The active sites are expected to be at the interface between Pd and the ReO_x clusters. Activation through only the carbonyl group would yield THF through the stepwise conversion of C=O to C–OH and then C–OH cleavage. The latter pathway would require a higher activation barrier energy for adsorption and hydrogenolysis of the C=O over a Re-Pd surface.

Another important point is that, notwithstanding extensive characterization, the specific nature of the most active sites is still unclear. Poor information is still available on the importance of the location or which oxidation valence is the most important to control the selectivity to BDO. Overall, there does not appear to be a consistent trend between the fraction of Re that has been reduced to Re^0 and the final selectivity to BDO.

Tentative mechanism

One of the most evident features is that in all formulations of bimetallic catalysts, either "as-prepared" or even after reduction at 450 °C, Re is not com-

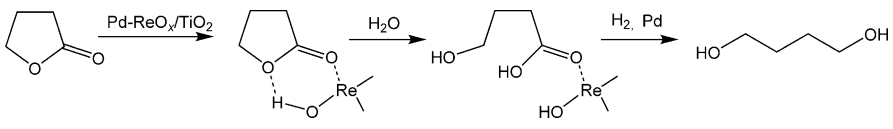

Scheme 2. Schematic reaction pathway to BDO.

Indeed, 2.6 wt%Re-Pd_{KCl}/DT51-SI and 1.9 wt%Re-Pd_{KCl}/DT51-CR, which are reduced to the same extent of 30% Re^0, gave very different selectivities of 78 and 26%, respectively. The 1.9 wt%Re-Pd_{KCl}/DT51-CR catalyst was particularly poorly active for both SUC transformation and GBL hydrogenation. This behavior is not related to the degree of reduction as 1.5 wt%Re-Pd_{KCl}/P25-CR in a highly reduced state (70% Re^0) was also poorly active. The catalysts that contained a lower fraction of Re^0 (0.9 wt%Re-Pd_{Cl}/P25-CR and 1.7 wt%Re-Pd_{Cl}/P25-CR) led to moderate BDO yields.

An important parameter might be the acid strength of the generated sites. It was shown that the acid strength was higher for OH sites bound to multiple oxophilic metal atoms in a threefold configuration rather than OH sites adsorbed in an on-top configuration on one oxophilic metal.[65] This hypothesis is consistent with the suggestion of a Re deposition by stacking using the CR protocol based on physicochemical characterizations. The ReO_x clusters may yield acid sites with a higher strength that might be less favorable for BDO selectivity.

Finally to conclude, we should be cautious that essentially all the characterizations of the solids were performed ex situ and might not be an exact representation of the structure and the interactions of these metals after reduction in the working catalysts under hydrothermal conditions. The question remains whether the metallic phases in the bimetallic catalysts are maintained during aqueous-phase processing. If we consider the structure of the bimetallic catalysts after synthesis, the reduced state might be different from that actually present in the hydrothermal environment under H_2. There are some indications in the literature that the reduction degree should remain intact. Characterization by in situ XANES in water showed that Re in PtRe at a high temperature of 225 °C remained reduced[44] and that Re in RhRe/C did not oxidize under aqueous-phase hydrogenolysis.[57] The elucidation of the active site and the reaction mechanism deserves further investigation.

Conclusions

Different techniques (XRD, TEM, high-angle annular dark-field scanning transmission electron microscopy, X-ray photoelectron spectroscopy, temperature-programmed reduction, H_2 chemisorption, and the cyclohexane dehydrogenation model reaction) were used to characterize ReO_x-Pd/TiO_2 catalysts prepared by using two different methods of Re promotion (successive impregnation or catalytic reduction) from three different monometallic Pd/TiO_2 catalysts. Significant interactions between the two metals were demonstrated, although without electronic modification. Monomeric structures of ReO_x were evidenced by high-angle annular dark-field scanning transmission electron microscopy everywhere over the catalyst. The mechanism proposed for the selective hydrogenation of succinic acid to 1,4-butanediol highlights the role of oxidized Re clusters bound to Pd in the activation of γ-butyrolactone, ring opening, and hydrogenation to 1,4-butanediol. It is also proposed that the different catalytic performances in the hydrogenation of succinic acid by bimetallic catalysts prepared by successive impregnation or catalytic reduction are a result of the different structures of ReO_x clusters on the Pd surface. In the catalysts prepared by successive impregnation, ReO_x was formed as islands, whereas in those prepared by catalytic reduction, the formation of multilayer ReO_x was orientated by stacking.

Experimental Section

Preparation of catalysts

The catalysts used in this study were TiO_2-supported Pd and Re-Pd catalysts. Two commercial supports were used: TiO_2 DT51 (specific surface area 88 $m^2 g^{-1}$, mean mesopore diameter 12 nm, supplied by Cristal) and TiO_2 P25 (specific area 50 $m^2 g^{-1}$, supplied by Degussa-Evonik). The Re-modified catalysts are referred to as bimetallic catalysts throughout the manuscript, although a real alloy between the components was not evidenced. They were prepared from the synthesized monometallic Pd catalysts. Ammonium perrhenate (NH_4ReO_4) was used as the source of Re.

The 2 wt%Pd_{Cl}/P25 catalyst was prepared using $PdCl_2$ as precursor salt by an impregnation method performed in an acidic aqueous medium (pH 1, HCl 32 wt%) as described previously.[20,21] After the impregnation step, the solvent was evaporated, and the solid was dried in an oven at 120 °C, treated by calcination under air at 300 °C for 4 h, and finally reduced in flowing H_2 (3.6 $L h^{-1}$) at 300 °C.

The 2 wt%Pd_{KCl}/P25 and 2 wt%Pd_{KCl}/DT51 catalysts were prepared by deposition–precipitation using K_2PdCl_4 as the precursor.[21] An appropriate amount of the precursor salt was slowly added to a suspension of the support (10 g) in water. After 30 min stirring, the pH was adjusted and maintained at pH 11 by the addition of KOH. The suspension was heated to reflux at 100 °C for 1 h. After cooling, the solid was collected by filtration and washed thoroughly several times by dispersing it in water (200 mL), decantation, and centrifugation until the supernatant had a neutral pH. The solid was dried under vacuum at 50 °C overnight, reduced in flowing H_2 (3.6 $L h^{-1}$) at 300 °C for 3 h, and finally passivated under 1 vol% O_2 in N_2 (1.8 $L h^{-1}$, 30 min).

Monometallic Re catalysts were prepared using aqueous solutions of NH_4ReO_4 as the precursor. The 1.9 wt%Re_{pH1}/P25 catalyst was prepared by impregnation of TiO_2 P25 in acidic medium (pH 1), evaporation, drying in an oven at 120 °C, and reduction at 450 °C in H_2 (to mimic the CR deposition),[20] whereas 3.1 wt%Re_{pHn}/DT51 was prepared using the same procedure, except the pH of the precursor aqueous solution was not adjusted (to mimic the SI deposition).

The supported Re-Pd bimetallic catalysts were prepared from the parent Pd catalysts by the addition of different amounts of Re using two different methods: SI and ex situ CR. In the SI method, an aqueous solution of a predetermined amount of the Re salt was added to a suspension of the parent Pd catalyst at RT. After 5 h stirring, the excess water was evaporated by using a rotary evaporator at 50 °C under vacuum. The sample was dried overnight at 50 °C under vacuum, reduced in H_2 flow at 450 °C, and finally passivated in 1 vol% O_2 in N_2. The CR deposition method relies on a surface redox reaction between adsorbed atomic hydrogen on Pd (Pd-H_{ads}) in the parent catalyst and the Re precursor according to the overall reaction [Eq. (1)]:

$$ReO_4^- + n\,Pd\text{-}H_{ads} + (8-n)\,H^+ \rightarrow (Pd)_n\text{-}Re^{(7-n)+} + 4\,H_2O \quad (1)$$

This method should direct the deposition of Re onto the pre-existing Pd particles.[66] The parent Pd/TiO_2 catalyst was placed in a fixed-bed reactor, and after purging with inert gas, the solid was reactivated at 300 °C for 1 h and then cooled under a H_2 flow (3.6 L h^{-1}). Then, the Re aqueous solution (acidified to pH 1 with HCl and degassed with an inert gas) was poured onto the Pd catalyst. The mixture was maintained for 1 h under H_2 bubbling at RT. The solution was filtered, and the catalyst was dried overnight at 100 °C in the fixed-bed reactor under H_2, before reduction in H_2 flow (3.6 L h^{-1}) at 450 °C. The reduced catalysts were allowed to cool under H_2. Once RT was reached, the catalyst was flushed with N_2, followed by slow exposure to air.

The SI catalysts were exposed to air and stored under Ar before they were used for characterization or a reaction test. The catalysts prepared by CR were stored in ambient air. They are denoted "as-prepared" bimetallic catalysts.

Characterization of catalysts

The actual bulk Pd and Re loadings in the catalysts were determined with an accuracy of ±0.1 wt% by ICP-OES by using an ACTIVA instrument (Horiba Jobin Yvon) after acid digestion with H_2SO_4, HCl, and HNO_3.

XRD patterns of the catalysts were recorded in the range $2\theta = 10$–$80°$ (scan step 0.03°, step time 2 s) by using a Bruker D5005 X-ray diffractometer and a CuK_α radiation source ($\lambda = 1.54056$ Å). Phase identification was made by comparison with the JCPDS database. Crystal sizes were estimated if possible using the Scherrer equation from the width at half maximum intensity.

TEM and STEM were conducted by using a JEOL 2010 instrument with a LaB6 source operated at 200 kV coupled to a Oxford Link ISIS instrument for microanalysis EDX spectroscopy and a JEOL 2010 FEG equipped with a field-emission gun operated at an acceleration voltage of 200 kV. ETEM was performed on some samples to achieve a better resolution (1.36 Å) by using a FEI TITAN G2 80–300 kV instrument. HAADF-STEM was performed in the STEM mode with EDX to obtain elemental analysis. Pd L and Re M lines that are free from interferences by signals from other elements were used to quantify the relative amounts of Pd and Re, respectively. For the analysis of individual particles, the electron beam was focused to a diameter close to the diameter of the particle under investigation. Typically, monometallic Pd catalysts were observed after the samples were suspended in ethanol, sonicated, and dispersed over a copper mesh grid with a carbon film coating, and ethanol was allowed to evaporate. As rhenium oxo species are formed that may be soluble in water or in ethanol upon exposing the bimetallic catalysts to air, the bimetallic catalysts were dispersed dry on the carbon film with a syringe.

The surface chemical composition and oxidation states of Pd and Re in catalyst samples were analyzed by XPS by using a hemispherical analyzer with a Kratos Axis Ultra^{DLD} spectrometer with a delay line detector and charge neutralization system. XPS spectra were collected by using a monochromated AlK_α X-ray source ($h\nu =$ 1486.6 eV). The BEs were referenced to the C 1s line at 284.5 eV. XPS profiles of "as-prepared" catalysts and after in situ pretreatment in O_2 or H_2 in a cell connected directly to the XPS chamber were analyzed. After pretreatment, the samples were cooled to RT and transferred without exposure to air into the ultra-high vacuum chamber (10^{-9} mbar). Peak fitting was achieved using CASA XPS software. Quantitative determinations were performed using the Vision KRATOS software. The Re $4f_{7/2}$ component of the Re 4f characteristic doublets for each species was used to determine the BE and the chemical state of the Re species. The Re 4d and Pd 3d peaks were used to calculate the Re/Pd atomic ratios.

H_2-TPR measurements were performed in a flow apparatus after in situ pretreatment under pure O_2 for 1 h at 300 °C and after cooling to RT before the reduction under a 1.0 vol% H_2/Ar gas mixture. The temperature range was 25–700 °C with a ramp of 5 °C min^{-1}. H_2 consumption during the reduction was detected by using an AutoChem II/Micromeritics apparatus using a thermal conductivity detector.

The metallic accessibility was measured by H_2 chemisorption using a pulsed technique at 70 °C as described previously[20] (Supporting Information). This temperature was chosen to avoid the formation of a β-hydride phase. Re does not chemisorb hydrogen under these conditions.

Activity in cyclohexane dehydrogenation to benzene was also used to characterize the metallic function. The reaction was performed under atmospheric pressure in a continuous flow reactor at 270 °C. An injection of cyclohexane (2 mL h^{-1}) was made using a calibrated motor-driven syringe. The partial pressures were 97 and 3 kPa for H_2 and cyclohexane, respectively. All measurements were performed with a total flow rate of 100 mL min^{-1} with 20 mg catalyst to ensure a conversion lower than 13%. Samples were first reactivated at 300 °C (3.6 L h^{-1} H_2). Analysis of products was performed by GC with a flame ionization detector by using a HP-PLOT Al_2O_3 column (50 m).

Hydrogenation experiments

SUC with a purity > 99% was purchased from Aldrich Chemical Co. All aqueous catalytic hydrogenation experiments were performed by using a 300 mL high-pressure batch reactor (Parr 4560) equipped with a magnetically driven impeller and a liquid sampling system described previously[18–21] (Supporting Information). The experiments were performed at 160 °C to favor the formation of BDO. Indeed, it has been described that to obtain a high BDO/THF ratio, the reaction should be preferably performed at temperature close to 150 °C, whereas temperatures close to 225–240 °C will achieve a higher THF/BDO ratio.[14,17,67]

Acknowledgements

The financial support for this work was provided by ANR (French Agence Nationale de la Recherche) within the Programme Chimie et Procédés pour le Développement Durable CP2D 2009 (HCHAIB). The authors acknowledge AXELERA for the support and the CLYM for guidance in the Ly-EtTEM project, which was financially supported by the CNRS, the Région Rhône-Alpes, the "Grand Lyon", and the French Ministry of Research and Higher Education.

Keywords: hydrogenation · palladium · rhenium · succinic acid · supported catalysts

[1] C. S. K. Lin, R. Luque, J. H. Clark, C. Webb, C. Du, *Biofuels Bioprod. Biorefin.* **2012**, *6*, 88–104.

[2] J. J. Beauprez, M. De Mey, W. K. Soetaert, *Process Biochem.* **2010**, *45*, 1103 – 1114.
[3] A. Cukalovic, C. V. Stevens, *Biofuels Bioprod. Biorefin.* **2008**, *2*, 505 – 529.
[4] C. Delhomme, D. Weuster-Botz, F. E. Kuhn, *Green Chem.* **2009**, *11*, 13 – 26.
[5] J. Xu, B. H. Guo, *Biotechnol. J.* **2010**, *5*, 1149 – 1163.
[6] S. E. Pedersen, J. G. Frye Jr., T. G. Attig, J. R. Budge, US 5 698 749, **1997**.
[7] M. A. Mabry, W. W. Prichard, S. B. Ziemecki, US 4 609 636, **1986**.
[8] U. G. Hong, S. Hwang, J. G. Seo, J. Yi, I. K. Song, *Catal. Lett.* **2010**, *138*, 28 – 33.
[9] U. G. Hong, J. Lee, S. Hwang, I. K. Song, *Catal. Lett.* **2011**, *141*, 332 – 338.
[10] U. G. Hong, S. Hwang, J. G. Seo, J. Lee, I. K. Song, *J. Ind. Eng. Chem.* **2011**, *17*, 316 – 320.
[11] U. G. Hong, H. W. Park, J. Lee, S. Hwang, I. K. Song, *J. Ind. Eng. Chem.* **2012**, *18*, 462 – 468.
[12] U. G. Hong, H. W. Park, J. Lee, S. Hwang, J. Yi, I. K. Song, *Appl. Catal. A* **2012**, *415 – 416*, 141 – 148.
[13] U. G. Hong, J. K. Kim, J. Lee, J. K. Lee, J. H. Song, J. Yi, I. K. Song, *Appl. Catal. A* **2014**, *469*, 466 – 471.
[14] K. H. Kang, U. G. Hong, Y. Bang, J. H. Choi, J. K. Kim, J. K. Lee, S. J. Han, I. K. Song, *Appl. Catal. A* **2015**, *490*, 153 – 162.
[15] J.-A. T. Schwartz, US 5478952, **1995**.
[16] R. E. Bockrath, D. Campos, J-A. T. Schwartz, R. T. Stimeck, US 6008384, **1999**.
[17] Z. Shao, C. Li, X. Di, Z. Xiao, C. Liang, *Ind. Eng. Chem. Res.* **2014**, *53*, 9638 – 9645.
[18] D. Pham Minh, M. Besson, C. Pinel, P. Fuertes, C. Petitjean, *Top. Catal.* **2010**, *53*, 1270 – 1273.
[19] B. K. Ly, D. P. Minh, C. Pinel, M. Besson, B. Tapin, F. Epron, C. Especel, *Top. Catal.* **2012**, *55*, 466 – 473.
[20] B. Tapin, F. Epron, C. Especel, B. K. Ly, C. Pinel, M. Besson, *Catal. Today* **2014**, *235*, 127 – 133.
[21] B. Tapin, F. Epron, C. Especel, B. K. Ly, C. Pinel, M. Besson, *ACS Catal.* **2013**, *3*, 2327 – 2335.
[22] J. Okal, *Appl. Catal. A* **2005**, *287*, 214 – 220.
[23] H. Iida, A. Igarashi, *Appl. Catal. A* **2006**, *303*, 192 – 198.
[24] J. F. Moulder, W. F. Stickle, P. E. Sobol, K. O. Bomben, *Handbook of X-ray Photoelectron Spectroscopy*, PerkinElmer Corporation, USA, **1992**, pp. 174 – 175.
[25] S. R. Bare, S. D. Kelly, F. D. Vila, E. Boldingh, E. Karapetrova, J. Kas, G. E. Mickelson, F. S. Modica, N. Yang, J. J. Rehr, *J. Phys. Chem. C* **2011**, *115*, 5740 – 5755.
[26] M. Rønning, D. G. Nicholson, A. Holmen, *Catal. Lett.* **2001**, *72*, 141 – 146.
[27] I. E. Wachs, G. Deo, M. A. Vuurman, H. Hu, D. S. Kim, J. M. Jehng, *J. Mol. Catal.* **1993**, *82*, 443 – 455.
[28] P. Arnoldy, E. M. Van Oers, O. S. L. Bruinsma, V. H. D. De Beer, J. A. Moulijn, *J. Catal.* **1985**, *93*, 231 – 245.
[29] M. A. Vuurman, D. J. Stufkens, A. Oskam, I. E. Wachs, *J. Mol. Catal.* **1992**, *76*, 263 – 285.
[30] C. A. González, A. N. Ardila, C. Montes de Correa, M. A. Martanez, G. Fuentes-Zurita, *Ind. Eng. Chem. Res.* **2007**, *46*, 7961 – 7969.
[31] H. C. Yao, M. Shelef, *J. Catal.* **1976**, *44*, 392 – 403.
[32] C. Micheaud, P. Marecot, M. Guerin, J. Barbier, *Appl. Catal. A* **1998**, *171*, 229 – 239.
[33] M. T. Schaal, J. Rebelli, H. M. McKerrow, C. T. Williams, J. R. Monnier, *Appl. Catal. A* **2010**, *382*, 49 – 57.
[34] A. Douidah, P. Marecot, S. Labruquere, J. Barbier, *Appl. Catal. A* **2001**, *210*, 111 – 120.
[35] G. Lafaye, C. Micheaud-Especel, C. Montassier, P. Marecot, *Appl. Catal. A* **2002**, *230*, 19 – 30.
[36] M. Guenin, M. Breysse, R. Frety, K. Tifouti, P. Marecot, J. Barbier, *J. Catal.* **1987**, *105*, 144 – 154.
[37] R. W. Maatman, P. Mahaffy, P. Hoekstra, C. Addink, *J. Catal.* **1971**, *23*, 105 – 118.
[38] J. A. Cusumano, G. W. Dembinski, J. H. Sinfelt, *J. Catal.* **1966**, *5*, 471 – 475.
[39] M. Boudart, A. Aldag, J. E. Benson, N. A. Doughary, C. G. Harkins, *J. Catal.* **1966**, *6*, 92 – 99.
[40] C. L. Pieck, P. Marecot, J. M. Parera, J. Barbier, *Appl. Catal. A* **1995**, *126*, 153 – 163.
[41] J. Sá, C. Kartusch, M. Makosch, C. Paun, J. A. van Bokhoven, E. Kleymenov, J. Szlatchenko, M. Nachtegaal, H. G. Manyar, C. Hardacre, *Chem. Commun.* **2011**, *47*, 6590 – 6592.
[42] A. Malinowski, W. Juszczyk, M. Bonarowska, J. Pielaszek, Z. Karpinski, *J. Catal.* **1998**, *177*, 153 – 163.
[43] Y. Sato, K. Terada, S. Hasegawa, T. Miyao, S. Naito, *Appl. Catal. A* **2005**, *296*, 80 – 89.
[44] J. Okal, W. Tylus, L. Kepinski, *J. Catal.* **2004**, *225*, 498 – 509.
[45] A. Ciftci, D. A. J. M. Ligthart, A. O. Sen, A. J. F. van Hoof, H. Friedrich, E. J. M. Hensen, *J. Catal.* **2014**, *311*, 88 – 101.
[46] A. S. Fung, P. A. Tooley, M. J. Kelley, D. C. Koningsberger, B. C. Gates, *J. Phys. Chem.* **1991**, *95*, 225 – 234.
[47] B. Mitra, X. Gao, I. E. Wachs, A. M. Hirt, G. Deo, *Phys. Chem. Chem. Phys.* **2001**, *3*, 1144 – 1152.
[48] S. Koso, H. Watanabe, K. Okumura, Y. Nakagawa, K. Tomishige, *Appl. Catal. B* **2012**, *111 – 112*, 27 – 37.
[49] S. Koso, H. Watanabe, K. Okumura, Y. Nakagawa, K. Tomishige, *J. Phys. Chem. C* **2012**, *116*, 3079 – 3090.
[50] Y. Amada, H. Watanabe, M. Tamura, Y. Nakagawa, K. Okumura, K. Tomishige, *J. Phys. Chem. C* **2012**, *116*, 23503 – 23514.
[51] T. Ebashi, Y. Ishida, Y. Nakagawa, S.-i. Ito, T. Kubota, K. Tomishige, *J. Phys. Chem. C* **2010**, *114*, 6518 – 6526.
[52] E. L. Kunkes, D. A. Simonetti, J. A. Dumesic, W. D. Pyrz, L. E. Murillo, J. G. Chen, D. J. Buttrey, *J. Catal.* **2008**, *260*, 164 – 177.
[53] D. J. King, L. Zhang, G. Xia, A. M. Karim, D. J. Heldebrand, X. Wang, T. Peterson, Y. Wang, *Appl. Catal. B* **2010**, *99*, 206 – 213.
[54] L. Ma, D. He, Z. Li, *Catal. Commun.* **2008**, *9*, 2489 – 2495.
[55] Y. Shinmi, S. Koso, T. Kubota, Y. Nakagawa, K. Tomishige, *Appl. Catal. B: Environmental* **2010**, *94*, 318 – 326.
[56] M. Chia, J. Pagan-Torres, D. Hibbits, Q. Tan, H. N. Pham, A. K. Datye, M. Neurock, R. J. Davis, J. A. Dumesic, *J. Am. Chem. Soc.* **2011**, *133*, 12675 – 12689.
[57] M. Chia, B. J. O'Neill, R. Allamino, P. J. Dietrich, F. H. Ribeiro, J. T. Miller, J. A. Dumesic, *J. Catal.* **2013**, *308*, 226 – 236.
[58] Y. Nakagawa, X. Ning, Y. Amada, K. Tomishige, *Appl. Catal. A* **2012**, *433 – 433*, 128 – 134.
[59] K. Chen, S. Koso, T. Kubota, Y. Nakagawa, K. Tomishige, *ChemCatChem* **2010**, *2*, 547 – 555.
[60] T. Buntara, I. Melian-Cabrera, Q. Tan, J. L. G. Fierro, M. Neurock, J. G. de Vries, H. J. Heeres, *Catal. Today* **2013**, *210*, 106 – 116.
[61] R. Burch, C. Paun, X.-M. Cao, P. Crawford, P. Goodrich, C. Hardacre, P. Hu, L. McLaughlin, J. Sa, J. M. Thompson, *J. Catal.* **2011**, *283*, 89 – 97.
[62] G. Beamson, A. J. Papworth, C. Philips, A. M. Smith, R. Whyman, *J. Catal.* **2011**, *278*, 228 – 238.
[63] M. Tamura, R. Tamura, Y. Takeda, Y. Nakagawa, K. Tomishige, *Chem. Eur. J.* **2015**, *21*, 3097 – 3107.
[64] L. Zhang, A. M. Karim, M. H. Engelhard, Z. Wei, D. L. King, Y. Wang, *J. Catal.* **2012**, *287*, 37 – 43.
[65] D. Hibbitts, Q. Tan, M. Neurock, *J. Catal.* **2014**, *315*, 48 – 58.
[66] F. Epron, C. Especel, G. Lafaye, P. Marecot, *Nanoparticles and Catalysis* (Ed.: D. Astruc), Wiley-VCH, Weinheim, **2008**, pp. 279 – 302.
[67] E. I. Du Pont De Nemours, US 6008384, **1999**.

Received: February 27, 2015
Published online on June 3, 2015